AD-A031 562 NAVAL RESEARCH LAB WASHINGTON D C F/G 4/1
CALCULATION OF THE IONOSPHERIC PHOTOELECTRON DISTRIBUTION FUNCT--ETC(U)
SEP 76 E S ORAN, D J STRICKLAND

UNCLASSIFIED NRL-MR-336 NL

END

DATE FILMED 12-76

NRL Memorandum Report 3361

Calculation of the Ionospheric Photoelectron Distribution Function

ELAINE S. ORAN

Plasma Dynamics Branch
Plasma Physics Division

and

D. J. STRICKLAND

Science Applications, Inc.
McLean, Virginia 22101

September 1976

NAVAL RESEARCH LABORATORY
Washington, D.C.

SECURITY CLASSIFICATION OF THIS PAGE (When Data Entered)

REPORT DOCUMENTATION PAGE

READ INSTRUCTIONS BEFORE COMPLETING FORM

1. REPORT NUMBER
NRL Memorandum Report 3361

2. GOVT ACCESSION NO.

3. RECIPIENT'S CATALOG NUMBER

4. TITLE (and Subtitle)
CALCULATION OF THE IONOSPHERIC PHOTOELECTRON DISTRIBUTION FUNCTION

5. TYPE OF REPORT & PERIOD COVERED
Interim report on a continuing NRL problem.

6. PERFORMING ORG. REPORT NUMBER

7. AUTHOR(s)
Elaine S. Oran and D. Strickland

8. CONTRACT OR GRANT NUMBER(s)
NRL-MR-3361

9. PERFORMING ORGANIZATION NAME AND ADDRESS
Naval Research Laboratory
Washington, D.C. 20375

10. PROGRAM ELEMENT, PROJECT, TASK AREA & WORK UNIT NUMBERS
NRL Problems A03-16 and 17

11. CONTROLLING OFFICE NAME AND ADDRESS
Office of Naval Research
Arlington, Virginia 22203

12. REPORT DATE
September 1976

13. NUMBER OF PAGES
54

14. MONITORING AGENCY NAME & ADDRESS(if different from Controlling Office)

15. SECURITY CLASS. (of this report)
UNCLASSIFIED

15a. DECLASSIFICATION/DOWNGRADING SCHEDULE

16. DISTRIBUTION STATEMENT (of this Report)
Approved for public release; distribution unlimited.

17. DISTRIBUTION STATEMENT (of the abstract entered in Block 20, if different from Report)

18. SUPPLEMENTARY NOTES

19. KEY WORDS (Continue on reverse side if necessary and identify by block number)
Photoelectron distribution function
Ionosphere
Electron flux
Electron scattering

20. ABSTRACT (Continue on reverse side if necessary and identify by block number)
We present calculations of the photoelectron flux in the ionosphere which have been obtained by solving the Boltzmann equation. The method is flexible enough to allow for a wide range of energy and angular dependences for both external and internal electron sources. Detailed comparisons of calculated and measured photoelectron fluxes show excellent agreement. We also show a series of solutions which indicate the sensitivity of the calculations to the solar zenith angle, isotropic versus forward peaked elastic scattering, and resolution of the energy and angular grids. At altitudes above

(Continues)

DD FORM 1 JAN 73 1473 EDITION OF 1 NOV 65 IS OBSOLETE
S/N 0102-014-6601

SECURITY CLASSIFICATION OF THIS PAGE (When Data Entered)

cont.

20. Abstract (continued)

300 km, the assumption of forward peaked scattering gives significantly greater anisotropies in the calculated flux. To determine grid sensitivity, ~~we show~~ results are obtained for energy grids containing 50 and 20 points between 2 and 90 ev and for angular grids containing 20, 10, and 4 points. Grids which are too coarse can lead to overall errors in the fluxes of a factor of two or larger.

CONTENTS

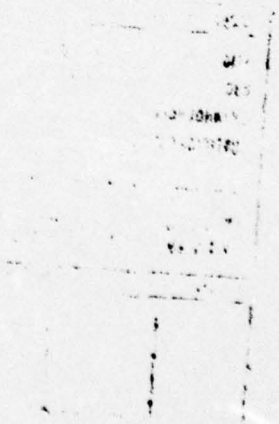

CALCULATION OF THE IONOSPHERIC PHOTOELECTRON DISTRIBUTION FUNCTION

I. INTRODUCTION

Through the process of photoionization, a fraction of the solar radiation which reaches the earth is transformed into electron kinetic energy. Subsequent collisions between the electrons formed by photoionization processes and the neutral particles produce the ambient electron and ion gas as well as heat the neutral atmosphere. The ambient electron, ion, and neutral gases may each be characterized by a Maxwellian distribution at a temperature from 300 - 4000 ^{o}K. Those electrons which are removed from the neutral molecules either directly through photoionization or through the collisional formation of secondaries are called "photoelectrons". They have energies substantially greater than the ones characterizing the Maxwellian electron gas and their distribution function can be described as an irregular high energy tail on the Maxwellian. The main source of heating the ambient thermal electrons occurs through their interaction with the photoelectrons.

The work presented below describes our effort to understand how energetic electrons are degraded and transported in the earth's atmosphere. We calculate a distribution function for the high energy photoelectrons which can also include the effects of electrons of even higher energies which come into the atmosphere along magnetic field lines. Our

Note: Manuscript submitted August 26, 1976.

goal is to describe in detail the redistribution of the energy of the electrons among the ambient thermal electrons, ions, and neutral particles. From this information we calculate atmospheric quantities, such as electron temperatures and densities of excited states, which are crucial to our ability to understand and predict the state of the ionosphere.

Photoelectrons can lose energy through a myriad of collisional processes which ionize or excite the neutrals. For O_2 and N_2, both rotational and vibrational states may also be excited. Excited species are important in the processes which control the chemical balance of the ionosphere and they contribute to the observed dayglow emissions. Electron-electron collisions and the excitation of plasma waves are responsible for heating the ambient thermal electron gas and subsequently the ion and neutral gas. Any calculation of the electron temperature requires a description of the heat transfer and conduction processes. Photoelectrons are responsible for the observed predawn heating of the ionosphere due to the influx of electrons along magnetic field lines. This occurs when the conjugate ionospheric region is in daylight. If we wish to properly account for all of these processes, we need to know the details of the atomic and molecular structure, the relevant interaction cross sections, and the plasma interactions.

Photoelectron transport calculations have been made by Nisbet (1968) and Swartz (1972), Nagy and Banks (1970) and Banks and Nagy (1970), Cicerone and Bowhill (1970, 1971), and most recently by Mantas (1975). The Nisbet method is based on diffusion theory and determines the photoelectron flux by solving a set of coupled flux equations. Escaping electrons are accounted for by including an additional loss term which

is separately calculated. Swartz modified this approach by directly including the flux divergence term. Nagy and Banks solved for the electron flux in a two-stream approximation and thus attempted to treat the high altitude transport properties of photoelectrons. Cicerone and Bowhill used a Monte Carlo method which follows the path of the individual particles. The limitations and problems inherent in each of these three approaches have been analyzed in detail by Cicerone et al. (1973). The Nisbet and Swartz method requires the calculation of a diffusion coefficient for electrons through the atmosphere which depends on the pitch angle distribution and on the details of the collisional scattering. A two-stream model such as Nagy and Banks' can omit the essential features of angular anisotropies in the particle distributions. A Monte Carlo method is in principle the most comprehensive and does not require any information a priori on the pitch angle distribution. It is limited, however, by its computer cost and core requirements.

The transport equation approach, such as that used by Mantas (1975) for photoelectrons and by Strickland et al. (1976) for auroral electrons, is currently the most feasible and versatile method. Below we show solutions of the Boltzmann equation which give the photoelectron distribution function. As a biproduct we find the population density of excited ionic and neutral states from which airglow emissions can be calculated. With minimal additional effort the effects of high energy particle fluxes, electric and magnetic field effects, and varying solar conditions can be included in the calculation. The numerical method is based on the one described by Strickland et al. (1976) for auroral

electrons and will be discussed in more detail in a later section. In this paper we will describe model calculations of the photoelectron distribution function and give some comparisons with observed spectra. Specific studies using these results, such as electron temperature, airglow calculations, or conjugate point effects are reserved for later papers.

II. THEORETICAL BACKGROUND

The photoelectron distribution function, $f(\bar{r}, \bar{v}, t)$, is found from the solution of the Boltzmann equation,

$$\frac{\partial f}{\partial t} + \underline{v}\cdot\nabla_{\underline{r}} f + \dot{\underline{v}}\cdot\nabla_{\underline{v}} f = Q(\underline{r}, \underline{v}, t) + \left.\frac{\partial f}{\partial t}\right|_c , \qquad (1)$$

where $\partial f/\partial t$ represents the local variation of f with time, the second term describes the change in f due to spatial gradients, the third term describes the presence of external forces, Q is the local production rate of primary electrons due to solar radiation, and $\partial f/\partial t|_c$ reflects the change in f due to elastic and inelastic collisions with other electrons, ions, and neutral constituents. For our present purposes we have introduced a number of simplifying assumptions which are described in the paragraphs below.

First, we assume that photoelectrons are transported predominately along magnetic field lines and that the atmosphere is horizontally stratified along these field lines. This approximation, which is good at middle and high latitudes, allows us to assume azimuthal symmetry

about a magnetic field line and also to write the spatial gradient in Eq. (1) as a derivative along a direction $\hat{z}$ which is parallel to $\underline{B}$. We then need to consider transport only along $\hat{z}$. The time derivative of the velocity, $\dot{\underline{v}}$, is proportional to the electric field, $\underline{E}$, and to $\underline{v} \times \underline{B}$,

$$\dot{\underline{v}} = - \frac{e}{m_e} \left[\underline{E} + \underline{v} \times \underline{B} \right] , \qquad (2)$$

where e is the charge on an electron and m_e is its mass. Since we consider transport only along $\hat{z}$ and assume no electric fields are present, this term does not contribute to Eq. (1).

Since interaction with the photoelectrons is the primary source of heating the ambient thermal electrons, we now consider how to include this in Eq. (1). Butler and Buckingham (1962), Itikawa and Aono (1966), and Perkins (1965) have looked in some detail at the way in which a charged particle loses energy as it moves through a thermal plasma. When we apply their work to the ionosphere, we conclude that energy loss to ions is negligible and that we only have to consider photoelectron-thermal electron interactions. Energy loss is due to the combined effects of two-body Coulomb collisions and the collective effect of Cerenkov emission of plasma waves. Schunk and Hays (1971) have expressed the energy loss of a high energy electron in a lower energy electron gas as

$$-\frac{dE}{dt} = \frac{\omega_p^2 e^2}{v} \begin{cases} \ell n \dfrac{m_e v^3}{\gamma \omega_p e^2}, & kT \ll E < \dfrac{m_e e^4}{2\hbar^2} \\ \ell n \dfrac{m_e v^2}{\hbar \omega_p}, & E > \dfrac{m_e e^4}{2\hbar^2}, \end{cases} \tag{3}$$

where E is the photoelectron energy,

$$v = \left(\frac{2\ kT}{m_e} \right)^{1/2} \tag{4}$$

is the photoelectron velocity, ω_p is the plasma frequency

$$\omega_p = \left(\frac{4\pi n_e e^2}{m_e} \right)^{1/2}, \tag{5}$$

n_e and T are the thermal electron number density and temperature, respectively, and $\ell n\ \gamma$ is Euler's constant. The second formula in Eq. (3) describes energy loss for those energies in which the deBroglie wavelength is greater than the classical distance of closest approach and a quantum mechanical treatment is required. Equation (3) is incorporated into Eq. (1) by the method described by Mantas (1975), who treats this loss process as an extra "friction" term which is added to $\dot{\underline{v}}$ in Eq. (2). Note that we are assuming a continuous energy loss of the photoelectrons to the ambient electrons and that the photoelectrons are not deflected in this process. We have included this process in the third term in Eq. (1).

We wish to solve for the flux, $\phi(t, z, E, \mu)$, which is related to the distribution function through

$$\phi(t, z, E, \mu) = v(E) f(t, z, E, \mu) \ . \tag{6}$$

Then for the assumptions we have just discussed, Eq. (1) becomes

$$\frac{1}{v}\frac{\partial \phi}{\partial t} + \mu \frac{\partial \phi}{\partial z} + \mu n_e \mathcal{L}(E)\left(\frac{\phi}{2E} - \frac{\partial \phi}{\partial E}\right) = \cdots \ , \tag{7}$$

where μ is the cosine of the pitch angle, the angle between $\underline{v}$ and $\underline{B}$. The function $\mathcal{L}(E)$ is

$$\mathcal{L}(E) = \begin{cases} -\dfrac{2\pi e^4}{E} \ln\left(\dfrac{2E}{\hbar\omega_p}\right), & \text{for } E > E_o \\ -\dfrac{2\pi e^4}{E} \ln\left(\dfrac{2^{3/2} E^{3/2}}{m_e^{1/2} \gamma e^2 \omega_p}\right), & \text{for } E < E_o \end{cases} \tag{8}$$

where $E_o \approx 14$ eV.

In the work described below we assume that the steady state distribution function gives an adequate description of the photoelectron flux and set $\partial\phi/\partial t = 0$. This is justified by the short decay time of the initial distribution compared to any changes in the source term which produces primary electrons. Such an assumption is even reasonably accurate over the sunset period, except in a small altitude range from which the sun is disappearing at that time. We also transform Eq. (7) to solve for ϕ as a function of τ, the electron scattering depth, which

is defined by

$$d\tau = \sum_{\ell} n_{\ell}(z)\sigma^{\ell}(E)dz \ , \tag{9}$$

where $n_{\ell}(z)$ is the number density and $\sigma^{\ell}(E)$ is the total scattering cross section for species ℓ. With these changes, Eq. (7) becomes

$$\mu \frac{d\phi}{d\tau}(\tau, E, \mu) = -\phi(\tau, E, \mu) + \frac{\mu n_e \mathcal{L}(E)}{\sum_{\ell} n_{\ell}(z)\sigma^{\ell}(E)} \left(\frac{\partial \phi}{\partial E} - \frac{\phi}{2E} \right)$$

$$+ \int \chi(\mu', \mu, E', E)\phi(\tau, E', \mu)dE'd\mu' \tag{10}$$

$$+ Q(\tau, E, \mu) \ ,$$

where μ' and μ are the cosines of the pitch angles associated with the incident and outgoing directions and E' and E are incident and outgoing electron energies. The function χ gives the probability of scattering from the initial to the final energy and direction. It can be written as

$$\chi = \sum_{\ell} r_{\ell}(E, \tau)R_{\ell}(\mu', \mu, E', E) \ , \tag{11}$$

where

$$r_{\ell}(E, \tau) = \frac{n_{\ell}(z)\sigma^{\ell}(E)}{\sum_{m} n_m(z)\sigma^{m}(E)} \ . \tag{12}$$

The collision term in Eq. (1), $\partial f/\partial t\big|_c$, appears now as the first and third term on the right hand side of Eq. (10). The first term is proportional to the number of particles leaving a volume element in phase space and the third term describes how particles are scattered into a volume element. We consider collisions between photoelectrons and neutral particles which we assume are in thermal equilibrium. Collisions with ions cause negligible loss of energy and electron collisions have already been included. The redistribution function, R, is related to the cross sections by

$$R_\ell(\mu',\ \mu,\ E',\ E) = \frac{\sum_j \sigma_j^\ell(\mu',\ \mu,\ E',\ E)}{\sigma^\ell(E)} \quad , \tag{13}$$

where the sum is over all processes and $\sigma^\ell(E)$ is a total cross section for the species ℓ. The scattering processes which we include are elastic scattering by neutrals and excitation and ionization of ground state neutral particles. We consider three neutral species, N_2, O_2, and O and the relevant cross sections are summarized in Appendix A.

The source function, $Q(\tau,\ E,\ \mu)$, is the number of electrons produced directly by solar photoionization. The important processes contributing to Q are included and the photon fluxes used are those given by Hinteregger (1970) and those tabulated by Donnelly and Pope (1973). The relevant portion of the solar spectrum has been divided into 90 bands and lines. More calculational details and the relevant ionization cross sections are summarized in Appendix B.

III. METHOD OF SOLUTION

Equation (10) can be converted to matrix form

$$\mu_i \frac{\partial \phi_{ni}}{\partial \tau_n} = - \phi_{ni} + \sum_\ell r_{\ell n} \sum_j A^\ell{}_{nij} \phi_{nj} + S_{ni}$$

$$- \frac{n_e \mu_i}{\sum_\ell n_\ell \sigma_{\ell n}} \mathcal{L}(E_n) \left(\frac{1}{E_{n-1} - E_n} + \frac{1}{2 E_n} \right) \phi_{ni}$$

$$+ \frac{n_e \mu_i \mathcal{L}(E_n)}{\left(\sum_\ell n_\ell \sigma_{\ell n} \right) \left(E_{n-1} - E_n \right)} \phi_{n-1,i} , \qquad (14)$$

where the indices i and n refer to pitch angle and energy, respectively, j runs over pitch angles, and ℓ runs over species. We have assumed that the flux is linear in μ and quadratic in ℓn E over the E, μ grid. At the highest energy level, E_1, the flux has a power law dependence

$$\phi(\tau, E > E_1, \mu) = \phi(\tau, E_1, \mu) \left(\frac{E}{E_1} \right)^{-\alpha} , \qquad (15)$$

where α is chosen to provide a smooth continuation of the incident flux above E_1. The source function, S, includes those primary electrons formed directly by photoionization which are described by Q as well as those created through the degradation of high energy electrons. A detailed description of this matrix representation is given in Strickland et al. (1976).

The integration routine CHEMEQ by Young and Boris (1973) has been used to integrate Eq. (14). For a given energy, we begin by specifying the downward flux at $\tau = 0$ and setting the upward fluxes equal to those

produced directly by solar photoionization in the upward direction. Integration proceeds for downward fluxes from $\tau = 0$ to τ_o, the depth at the lower boundary. The solutions are stored over a preselected τ-grid. Starting with an upward flux of zero at τ_o, integration is then performed for upward fluxes from τ_o to 0 using as downward fluxes the previously stored values. The upward fluxes are stored on the same τ-grid used for storing downward values. This completes the first of several iterations needed to achieve convergence. Through a technique which projects the iterated solutions to their final values, as few as three or four iterations achieve excellent convergence to the final answer. The source term Q is evaluated by using a solar deposition routine written by T. R. Young and described in Oran et al. (1974).

The FORTRAN routines which solve Eq. (14) have been run on a 360/91 computer. For a test case of 50 energies (.5 to 120 eV) and 10 pitch angles, we require about 2 minutes to evaluate all of the R-matrices for the three neutral species. These are stored since they need to be evaluated only once for a specified E and μ grid. The final program, PHOTO, uses the R-matrices and the primary electron data to solve for the photoelectron fluxes. This requires another two minutes or less of computer time and requires ~ 450 K-bytes of storage. The times given include those required for a sizable amount of I/O. The program is flexible enough so that both ΔE and $\Delta\mu$ can vary throughout the range of energies and pitch angles. Thus we can easily look at one particular energy range on a much finer grid scale. Furthermore, if there are core storage problems the program can be run in tandem, where calculations

from higher energies are used as initial conditions for lower energy calculations.

In the next section we define a "standard" calculation for specified physical conditions and show how it is affected by changing physical parameters as well as parameters peculiar to the numerical scheme and choice of grids. As an initial test of the method, we compare a typical calculation with rocket and satellite measurements of photoelectron fluxes. The calculations in the next section look in detail at fluxes below 100 eV. We note, however, that the numerical scheme is capable of treating much higher energy electrons, such as those in the keV range describing auroral electrons (Strickland et al., 1976).

IV. RESULTS

We have two goals in presenting the calculations in this section. First, we wish to show that the theoretical and numerical techniques outlined in Sections II and III produce realistic results. We do this by choosing a "standard" calculation and showing that it is in good agreement with observed photoelectron fluxes. Second, we show the sensitivity of our calculations to variations in the important physical parameters and also to the internal parameters controlling the numerical calculation. More detailed comparisons to observations and further studies using these results will be described in subsequent papers.

A. Standard Calculation -- Qualitative Comparison to Measurements

Our "standard" calculation is for a zenith angle, χ, equal to 48° and a neutral atmosphere which is described by a Jacchia (1971) model with an exospheric temperature, T_{∞}, equal to 900 $^{\circ}$K. The neutral

number densities and the assumed ambient electron density are shown in Fig. 1. The primary electron spectra, which result directly from photoionization by solar radiation, is typical of low-medium solar conditions. We have shown this in Fig. 2 for several altitudes. For this photoelectron calculation, we have assumed that the primary flux is produced isotropically in pitch angle. In the standard calculation we have evaluated the equilibrium photoelectron fluxes at 2.5 eV intervals from 100 eV to 10 eV and at 2 eV intervals below this energy. At each energy and altitude, the flux is calculated for ten evenly spaced values of the cosine of the pitch angle from 1 (down the field lines) to -1 (up the field lines). The values of μ do not have to be evenly spaced and can vary depending on the resolution we require. The spacing in altitude is exponential and we have arbitrarily chosen to look at 115 to 750 km. For all of the calculations presented below, the incoming flux at the highest altitude has been set to zero. The effects of high energy particle precipitation will be discussed in another paper.

Figures 3a-f compare measured and the standard calculated photoelectron fluxes for selected altitudes from $\sim$ 120 km to $\sim$ 600 km. The vertical axes show the total flux divided by 4π. No attempt has been made here to reproduce the neutral atmosphere, electron density, or the solar conditions characteristic of any particular dataset. The observations are those of Knudsen and Sharp (1972), Galperin et al. (1972), and Doering et al. (1970, 1975, and 1976). We will not give a detailed evaluation of the accuracy of the data, though we note that the 1970 and 1972 observations are less accurate at low altitudes and low energies due to the photon-produced background counts. The later Doering et al.

fluxes (1975, 1976) are the most accurate measurements although they are inaccurate at energies above 60 eV due to stray photons and cosmic ray counts. The dip in observed fluxes in the low energy range (Doering, 1975) is shown in Fig. 3d. Doering et al. (1976) has explained that this is erroneous and the most recent data, such as shown in Fig. 3c for 180 - 190 km, agrees much better with the theoretical calculations. We note that the shape and magnitude of the flux at $\sim$ 250 km agrees quite well with Victor's calculations (1975) which do not include transport.

Below $\sim$ 250 km, the photoelectron flux is isotropic in pitch angle for all energies. At these low altitudes collision frequencies are high enough so that any initial directional preference is soon eliminated. Figures 4a-d show the flux as a function of pitch angle for selected energies at a fixed altitudes. At $\sim$ 400 km, Fig. 4c, the flux moving up the field line can be several orders of magnitude larger than the downward flux. It is at these F-region altitudes and above where both transport and anisotropy effects are important in a description of photoelectrons. Figures 5a and b show the variation of the flux as a function of pitch angle at several altitudes for 20 and 40 eV electrons. For completeness, we show total flux vs altitude for fixed energies in Fig. 6 and total upward and total downward flux vs altitude for fixed energies in Fig. 7a and b.

B. Numerical Sensitivity Tests

The calculations described below show the effect of varying parameters which describe the physical environment as well as those which

control the details of the numerical method.

The effect on the photoelectron flux due to an increase in zenith angle is most important at low altitudes. Figures 8a and b compare the calculated flux for three zenith angles, $\chi = 0^{o}$, 48^{o}, and 90^{o} at 119 and 545 km. The $\chi = 0^{o}$ and the $\chi = 90^{o}$ calculations have assumed Jacchia (1971) neutral atmospheres characterized by $T_{\infty} = 1100^{o}$ K and 870^{o} K respectively. The $\chi = 48^{o}$ neutral atmosphere was shown in Fig. 1 and it corresponds to $T_{\infty} = 900^{o}$K.

The thermal electron gas heating rate is found directly from the photoelectron flux using

$$Q_e(z) = \int_{E_o}^{E_{max}} \frac{dE}{ds} \Phi^T(E,z)dE \,, \qquad (16)$$

where dE/ds is given by Eq. (3) and Φ^T as in the total photoelectron flux at altitude z. The basic requirement on E_o, the lower limit of the integral, is that $E_o \gg kT$, where T is the ambient electron temperature. In the present calculation we have set $E_o = 1.0$ eV. This heating rate is shown in Fig. 9 for the three zenith angles mentioned above.

The assumption of isotropic elastic scattering is common in photoelectron calculations and we have made several tests to evaluate its validity. The standard calculation assumes that the scattering of primary electrons is forward peaked (see Strickland et al., 1976, for details). An isotropic distribution is assigned to the secondaries produced. For altitudes below 250 km, any anisotropies in the flux are removed by the high collision frequencies. Above this altitude, the effects of assuming purely isotropic scattering are apparent in the

magnitude of the total flux, but more pronounced in the pitch angle distribution. Figures 10a and b, and Fig. 11a and b compare the standard calculation with one that assumes isotropy in elastic scattering. As we would expect, the photoelectron fluxes show less variation in pitch angle when isotropic scattering is assumed.

We now consider the resolution in pitch angle which is required to get accurate solutions. We have calculated photoelectron fluxes with three different μ grids that contain 4, 10, and 20 points. For an energy grid, we have used a 20 energy point grid with $\Delta E = 5$ eV from 90 to 5 eV. The results are shown in Figs. 12 and 13. We conclude that changing the μ grid will not substantially alter either the shape or magnitude of the averaged flux. From Figs. 13 we see that the 4 point grid ($\mu = +1, 0.5, -0.5, -1$) gives essentially the same answers at these values of μ as the 10 or 20 point grids, although the points are too far apart to construct the true shape of flux vs μ when anisotropies occur. The 10-point grid does give essentially identical answers to the finer grid.

The standard calculation, which has a finer energy grid ($\Delta E = 2.5$ eV) and 10 points in the μ grid, is also shown on Figs. 12 and 13. At low altitudes the magnitude of the curves will be altered significantly by greater energy resolution. Figure 12b shows more structure appearing as the energy resolution is increased. The differences in magnitude above 60 eV are due to the different limits the calculation. The standard was calculated to 120 eV to insure accuracy

at 90 eV. The 20 energy test calculations were only to 90 eV. A 100-point energy test differs from the 50 energy standard calculation by a maximum of 5%, indicating that the 50 energy calculation is accurate enough to give the correct magnitude and energy for the flux.

V. CONCLUSION

We have presented the details of our calculation of the ionospheric photoelectron distribution function. Since we solve the Boltzmann equation, non-local effects are included and the results are valid throughout the D-, E-, and F- regions. The method of solution is computationally fast and accurate so that a number of important ionospheric studies are possible. Future work will look at phenomena such as high altitude escape fluxes, airglow, electron temperatures, and the effects of incoming electron fluxes in the ionosphere.

Acknowledgements

We would like to thank Jack Davis, Paul Julienne, George Schulz, and Marnix Van der Wiel for their help in determining the cross sections. We would also like to thank Ted Young and Dan Stein for their help in programming these calculations. Finally, we would like to thank Tim Coffey and Darrell Strobel for their encouragement.

This work was sponsored by the Naval Air Systems Command and the Office of Naval Research.

Appendix A

Electron Impact Cross Sections

The elastic cross sections for N_2, O_2 and O are shown on Figs. 14, 15, and 16, respectively. For O, the total and differential elastic scattering has been taken from Blaha and Davis (1975). The values of Shyn et al. (1972) have been used for N_2. The O_2 values have been obtained from Trajmar et al. (1972), Watson (1967) and Dehmel (1976). These cross sections are consistent with those found by subtracting the total inelastic cross section from the measured total scattering cross section. The method by which the differential inelastic cross section is incorporated in the model has been discussed in Strickland et al. (1976). References are given in Tables I, II, and III.

Table I - Inelastic Cross Sections for N_2

State	Reference
$^3\Sigma$	Winters (1966); P. S. Julienne (private communication)
$A\ ^3\Sigma_u^+$	Borst (1972)
$B\ ^3\Pi_g$	Stanton and St. Johns (1969); Chung and Lin (1972)
$C\ ^3\Pi_u$	Finn et al. (1972); Aarts and deHeer (1969)
Vibration	Schulz (1964); Engelhardt et al. (1964)
$W\ ^3\Delta_u$	Chung and Lin (1972); normalized to Chutjin et al. (1973)
$a\ ^1\Pi_g$	Green and Stolarski (1972)
$b\ ^1\Pi_u$	Green and Stolarski (1972)
$b\ ^1\Sigma_u^+$	Green and Stolarski (1972)
Rydbergs	Green and Stolarski (1972)
Ionization	Rapp and Englander-Golden (1965)

Table II - Inelastic Cross Sections for O_2

State	Reference
Vibration	Schulz and Dowell (1962); Hake and Phelps (1967); Trajmar et al. (1971); Trajmar et al. (1972); Wong et al. (1973)
a $^1\Delta_g$	Trajmar et al. (1971)
b $^1\Sigma_g^+$	Trajmar et al. (1971)
A $^3\Sigma_u^+$	Watson et al. (1967)
b $^3\Sigma_u^-$	Trajmar et al. (1972)
"9.9" Feature	Watson et al. (1967)
Rydbergs	Watson et al. (1967)
Ionization	Watson et al. (1967); Silverman and Lassettre (1957); Kieffer and Dunn (1966) Rapp et al.

Table III - Inelastic Cross Sections for O

State	Reference
^1D	Henry et al. (1969)
^1S	Henry et al. (1969)
^5S	Davis et al. (1975); Julienne and Davis (1976)
^3S	Davis et al. (1975); Julienne and Davis (1976)
$(3s)\ ^3D$ } Rydberg	Davis and Blaha (1976)
$(3s)\ ^1D$ } Rydberg	Davis and Blaha (1976)

Appendix B

Calculation of Primary Electron Spectrum

The electrons produced directly by solar photoionization of the ambient neutral particles in the atmosphere will be referred to as "primaries". The expression

$$q_{\ell,i}\left(z, E - I_{\ell,i}\right) = n_{\ell}(z)\sigma^{ion}_{\ell,i}(E)\phi_{\infty}(E)e^{-\sum_m \sigma^T_m(E)\int_z^{\infty} n_m(s)ds} \qquad \text{(B-1)}$$

gives the number of primaries produced at altitude z by solar radiation of energy E ionizing neutral species ℓ to ionization state i. The energy of the primaries produced is $E - I_{\ell,i}$, where $I_{\ell,i}$ is the ionization potential of ionization state i of neutral species ℓ, $\sigma^{ion}_{\ell,i}(E)$ is the corresponding ionization cross section, and $n_{\ell}(z)$ is the density of ℓ at altitude z. The solar radiation, characterized by the flux $\phi_{\infty}(E)$, is attenuated as it penetrates the earth's atmosphere. This process is represented by the exponential factor in which σ^T_m is the total absorption cross section of neutral species m and the integral is taken from the altitude point z along the line of sight to the sun.

The atmospheric species are ionized by radiation with energies down to 1026 Å. Characteristic fluxes for these energies for various solar conditions have been culled from Hinteregger (1970), Donnelly and Pope (1973), Swider (1969), Banks and Kocharts (1973) and Smith and Gottlieb (1974). Total absorption, ionization, and

dissociative ionization cross sections in the energy range 1 - 1026 Å have been tabulated from the references given in Table IV. We have included ionization from the neutral ground state to a number of singly positive excited states of the ion. These have been listed in Table V. A typical primary spectra is shown in Fig. 2.

Table IV

References for Photoionization and Absorption Cross Sections

Species	References	Comments
N_2	Hubbell (1971)	X-rays: $\sigma(N_2) \approx 2 \times \sigma(N)$.
	Lee et al. (1973)	Total absorption, 180 - 700 Å.
	Cook and Metzger (1964)	Total absorption and ionization, 600 - 1000 Å.
	Wight et al. (1976)	Dissociative ionization rates, 20 - 60 eV.
	Stolarski and Johnson (1972)	General compilation
	Hudson (1971)	Compilation and evaluation.
O_2	Hubbell (1971)	X-rays: $\sigma(O_2) \approx 2 \times \sigma(O)$.
	Lee et al. (1973)	
	Blake and Carver (1965)	Partial photoionization cross sections.
	Cook and Metzger (1964)	Total absorption and ionization, 6000 - 1000 Å.
	Matsunaga and Watanabe (1967)	Absorption and photoionization, 580 - 1070 Å.
	Fryar and Browning (1973)	Dissociative ionization for 304 and 584 Å.
	Stolarski and Johnson (1972)	General compilation
	Hudson (1971)	Compilation and evaluation.
O	Hubbell (1971)	X-rays.
	Henry (1967, 1970)	Partial photoionization cross sections.

Table V - Ionization States Included

Species	Ionization State
N_2	$X\ ^2\Sigma_g^+$
	$A\ ^2\Pi_u$
	$B\ ^2\Sigma_u^+$
	$E\ ^2\Sigma_g^+$
	$N + N^+$
O_2	$X\ ^2\Pi_g$
	$a\ ^4\Pi_u + A\ ^2\Pi_u$
	$b\ ^4\Sigma_g^-$
	$B\ ^2\Sigma_g^-$
	$c\ ^4\Sigma_u^-$
	$O + O^+$
O	^4S
	^2D
	^2P
	^4P
	^2P

REFERENCES

Aarts, J. F. M., and F. J. deHeer, Emission Cross Sections of the Second Positive Group of Nitrogen Produced by Electron Impact, Chem. Phys. Letters, 4, 116, 1969.

Banks, P. M., and G. Kocharts, Aeronomy, Vol. A, Chapter 7, Academic Press, London, 1973.

Banks, P. M., and A. F. Nagy, Concerning the Influence of Elastic Scattering upon Photoelectron Transport and Escape, J. Geophys. Res., 75, 1902, 1970.

Blaha, M., and J. Davis, Elastic Scattering of Electrons by Oxygen and Nitrogen at Intermediate Energies, Phys. Rev. A, 12, 2319, 1975.

Blake, A. J., and J. H. Carver, Partial Photoionization Cross Sections for Molecular Oxygen, Physics Letters, 19, 387, 1965.

Borst, W. L., Excitation of Several Important Metastable States of N_2 by Electron Impact, Phys. Rev., A5, 648, 1972.

Butler, S. T., and M. J. Buckingham, Energy Loss of a Fast Ion in a Plasma, Phys. Rev., 126, 1, 1962.

Chung, S. and C. C. Lin, Excitations of the Electronic States of the Nitrogen Molecule by Electron Impact, Phys. Rev., A6, 988, 1972.

Chutjin, A., D. C. Cartwright, and S. Trajmar, Excitation of the $W^3\Delta_u$, $w^1\Delta_u$, $B^3\Sigma_u^-$, and $a^1\Sigma_u^-$ States of N_2 by Electron Impact, Phys. Rev. Letters, 30, 195, 1973.

Cicerone, R. J., and S. A. Bowhill, Photoelectron Escape Fluxes Obtained by a Monte Carlo Technique, Radio Sci., 5, 49, 1970.

Cicerone, R. J., and S. A. Bowhill, Photoelectron Fluxes in the Ionosphere Computed by a Monte Carlo Method, J. Geophys. Res., 76, 8299, 1971.

Cicerone, R. J., W. E. Swartz, R. S. Stolarski, A. F. Nagy, and J. S. Nisbet, Thermalization and Transport of Photoelectrons: A Comparison of Theoretical Approaches, J. Geophys. Res., 78, 6709, 1973.

Cook, G. R., and P. H. Metzger, Photoionization and Absorption Cross Sections of O_2 and N_2 in the 600-1000 Å Region, J. Chem. Phys., 41, 321, 1964.

Davis, J., P. C. Kepple, and M. Blaha, Distorted Wave Calculations for Multiply Charged Nitrogen and Oxygen, J. Quant. Spectrosc. Radiat. Transfer, 15, 1145, 1975.

Davis, J., and M. Blaha, Electron Collision Excitation of Metastable Levels in NI, NII, OI, OII, OIII, submitted to Phys. Rev. A, 1976.

Dehmel, R. C., M. A. Fineman, and D. R. Miller, Angular Scattering of Low-Energy Electrons by Atomic and Molecular Oxygen, Argon, and Helium, Phys. Rev., A, 13, 115, 1976.

Doering, J. P., William G. Fastie, and P. D. Feldman, Photoelectron Excitation of N_2 in the Day Airglow, J. Geophys. Res., 75, 4787, 1970.

Doering J. P., W. K. Peterson, C. O. Bostrom, and J. C. Armstrong, Measurement of Low Energy Electrons in the Day Airglow and Day Side Auroral Zone from Atmosphere Explorer C, J. Geophys. Res., 80, 3934, 1975.

Doering, J. P., W. K. Peterson, C. O. Bostrom, and T. A. Potemra, High Resolution Daytime Photoelectron Energy Spectra from AE-E, Geophys. Res. Lett., 3, 129, 1976.

Donnelly, R. F., and J. H. Pope, The 1-3000 Å Solar Flux for a Moderate Level of Solar Activity for Use in Modeling the Ionosphere and Upper Atmosphere, NOAA Tech. Rept. ERL 276-SEL 25, 1973.

REFERENCES (cont.)

Engelhardt, A. G., A. V. Phelps, and C. G. Risk, Determination of Momentum Transfer and Inelastic Collision Cross Sections for Electrons in Nitrogen Using Transport Coefficients, Phys. Rev., 135, 1566, 1964.

Finn, T. G., J. F. M. Aarts, and J. P. Doering, High Energy Resolution Studies of Electron Impact Optical Excitation Functions I. The Second Positive System of N_2, J. Chem. Phys., 56, 5632, 1972.

Fite, W. L. and R. T. Brackmann, Ionization of Atomic Oxygen on Electron Impact, Phys. Rev., 113, 815, 1959.

Fryar, J., and R. Browning, Molecular Photoionization at 584 Å and 304 Å, Planet. Space Sci., 21, 709, 1973.

Galperin, Yu. I., M. Dymek, I. Kutiev, T. M. Mulyarchik, K. B. Serofionov, F. C. Shuiskaya, and A. Wernik, Spectra of Ionospheric Photoelectrons and Their Transport from the Conjugate Ionosphere, Rep. Acad. Sci., USSR Inst. Space Res., #107, 1972.

Green, A. E. S. and R. S. Stolarski, Analytic Models of Electron Impact Excitation Cross Sections, J. Atmos. Terr. Phys., 34, 1703, 1972.

Hake, R. D., Jr. and A. V. Phelps, Momentum Transfer and Inelastic Collision Cross Sections for Electrons in O_2, CO, and CO_2, Phys. Rev., 158, 70, 1967.

Henry, R. J. W., Photoionization Cross-Sections for Atomic Oxygen, Planet. Space Sci., 15, 1747, 1967.

Henry, R. J. W., P. G. Burke, and A. L. Sinfailam, Scattering of Electrons by C, N, O, N^+, O^+, and O^{++}, Phys. Rev., 178, 218, 1969.

Henry, R. J. W., Photoionization Cross Sections for Atoms and Ions of Carbon, Nitrogen, Oxygen, and Neon, Astro. J., 161, 1153, 1970.

Hinteregger, H. E., The Extreme Ultraviolet Solar Spectrum and its Variation During a Solar Cycle, Ann. Geophys., 26, 547-554, 1970.

REFERENCES (cont.)

Hubbell, J. H., Survey of Photon-Attenuation-Coefficient Measurements 10 eV to 100 GeV, Atomic Data, 3, 241, 1971.

Hudson, R. D., Critical Review of Ultraviolet Photoabsorption Cross Sections for Molecules of Astrophysical and Aeronomic Interest. Rev. Geophys. Space Phys., 9, 305, 1971.

Itikawa, Yukikazu, and Osamu Aono, Energy Change of a Charged Particle Moving in a Plasma, Phys. Fluids, 9, 1259, 1966.

Jacchia, L. G., Revised Static Models of the Thermosphere and Exosphere with Empirical Temperature Profiles, Spec. Rep. 332, Smithsonian Astrophys. Obs., Cambridge, Mass., 1971.

Julienne, P. S., and J. Davis, Cascade and Radiation Trapping Effects on Atmospheric Atomic Oxygen Emission by Electron Impact, J. Geophys. Res., 81, 1397, 1976.

Kieffer, L. J. and G. H. Dunn, Electron Impact Ionization Cross-Section Data for Atoms, Atomic Ions, and Diatomic Molecules I. Experimental Data, Rev. Mod. Phys., 38, 1, 1966.

Knudsen, W. C., and G. W. Sharp, Eclipse and Noneclipse Differential Photoelectron Flux, J. Geophys. Res., 77, 1221, 1972.

Lee, L. C., R. W. Carlson, D. L. Judge, and M. Ogawa, J. Quant. Spectrosc. Radiat. Transfer, 13, 1023, 1973.

Mantas, G. P., Electron Collision Processes in the Ionosphere, Aeronomy Report No. 54, Aeronomy Laboratory, Dept. of Electrical Engineering, University of Ill., Urbana, Ill., 1973.

Mantas, G. P., Theory of Photoelectron Thermalization and Transport and in the Ionosphere, Planet. Space Sci., 23, 337, 1975.

Mantas, G. P., and S. A. Bowhill, Calculated Photoelectron Pitch Angle and Energy Spectra, Planet. Space Sci., 23, 355, 1975.

REFERENCES (cont.)

Matsunaga, F. M., and K. Watanabe, Total and Photoionization Coefficients and Dissociation of O_2 in the 580-1070 Å Region, Sci. Light, 16, 31, 1967.

Mukai, T. and K. Hirao, Rocket Measurement of the Differential Energy Spectrum of the Photoelectrons, J. Geophys. Res., 78, 8395, 1973.

Nagy, A. F., and P. M. Banks, Photoelectron Fluxes in the Ionosphere, J. Geophys. Res., 75, 6260, 1970.

Nisbet, J. S., Photoelectron Escape from the Ionosphere, J. Atmos. Terr. Phys., 30, 1257, 1968.

Oran, E. S., T. R. Young, D. V. Anderson, T. P. Coffey, P. C. Kepple, A. W. Ali, and D. F. Strobel, A Numerical Model of the Midlatitude Ionosphere, NRL Memorandum Report 2839, Naval Research Lab., Wash., D. C., 1974.

Perkins, Francis, Motion of a Test Particle in a Plasma, Phys. Fluids, 8, 1361, 1965.

Rapp, D., and P. Englander-Golden, Total Cross Sections for Ionization and Attachment in Gases by Electron Impact II. Negative Ion Formation, J. Chem. Phys., 43, 1480, 1965.

Rapp, D., P. Englander-Golden, and D. D. Briglia, Cross Sections for Dissociative Ionization of Molecules by Electron Impact, J. Chem. Phys., 42, 4081, 1965.

Rothe, E. W., L. L. Marino, R. H. Neynaber, and S. M. Trujillo, Electron Impact Ionization of Atomic Hydrogen and Atomic Oxygen, Phys. Rev., 125, 582, 1962.

Schulz, G. J., Vibrational Excitation of N_2, CO and H_2 by Electron Impact, Phys. Rev., 135, 988, 1964.

Schulz, G. J., and J. T. Dowell, Excitation of Vibrational Electronic Levels in O_2 by Electron Impact, Phys. Rev., 128, 174, 1962.

REFERENCES (cont.)

Schunk, Robert W., and Paul B. Hays, Photoelectron Energy Losses to Thermal Electrons, Planet. Space Sci., 19, 113, 1971.

Shyn, T. W., R. S. Stolarski, and G. R. Caregman, Angular Distribution of Electrons Elastically Scattered from N_2, Phys. Rev. A., 6, 1002, 1972.

Silverman, S. M., and E. N. Lassettre, Electronic Collision Cross Sections, for Oxygen at Excitation Energies above 10 Volts, Rep. No. 7, Ohio State Dep. Chem. Sci., 1957.

Smith, Elske V. P., and David M. Gottlieb, Solar Flux and Its Variations, Space Sci. Rev., 16, 771, 1974.

Stanton, P. N. and R. M. N. St.Johns, Electron Excitation of the First Positive Bands of N and of First Negative and Meinel Bands of N_2, J. Opt. Soc. Am., 59, 252, 1964.

Stolarski, R. S., and N. P. Johnson, Photoionization and Photoabsorption Cross Sections for Ionospheric Calculations, J. Atmos. Terr. Phys., 34, 1691, 1972.

Strickland, D. J., and P. C. Kepple, Preliminary Report on the Transport and Production of Energetic Electrons in Auroras, N.R.L. Memorandum Report 2779, Naval Research Lab., Wash., D.C., 1974.

Strickland, D. J., D. L. Book, T. P. Coffey, and J. A. Fedder, Transport Equation Techniques for the Deposition of Auroral Electrons, J. Geophys. Res., 81, 2755, 1976.

Swartz, W. E., Electron Production, Recombination and Heating in the F Region of the Ionosphere, Sci. Rep. 381, Ionosphere Res. Lab., Pa. State Univ., University Park, 1972.

Swider, W., Jr., Ionization Rates Due to Attenuation of 1-100 Å Nonflare Solar X-Rays in the Terrestrial Atmosphere, Rev. of Geophys., 7, 573, 1969.

Trajmar, S., D. C. Cartwright, and W. Williams, Differential and Integral Cross Sections for Electron Impact Excitation of the a $^1\Delta_g$ and b $^1\Sigma_g^+$ States of O_2, Phys. Rev., A, 4, 1482, 1971.

Trajmar, S., W. Williams, and A. Kupperman, Angular Dependence of Electron Impact Excitation Cross Sections of O_2, J. Chem. Phys., 56, 3759, 1972.

Victor, G. A., K. Kirby-Docken, and A. Dalgarno, Calculations of the Equilibrium Photoelectron Flux in The Thermosphere, Preprint No. 453, Center for Astrophysics, Harvard College Observatory and Smithsonian Astrophysical Observatory, 1975.

Watson, C. E., V. A. Dulock, Jr., R. S. Stolarski, and A. E. S. Green, Electron Impact Cross Sections for Atmospheric Species III, Molecular Oxygen, J. Geophys. Res., 72, 3961, 1967.

Wedde, T. and T. G. Strand, Scattering Cross Sections for 40 eV to 1 keV Electrons Colliding Elastically with Nitrogen and Oxygen, J. Phys. B: Atom. Molec. Phys., 7, 1091, 1974.

Wight, G. R., M. J. Van der Wiel, and C. E. Brion, Dipole Excitation, Ionization and Fragmentation of N_2 and CO in the 10-60 eV region, J. Phys. B., 9, 675, 1976.

Winters, H. F., Ionic Absorption and Dissociation Cross Sections for Nitrogen, J. Chem. Phys., 44, 1472, 1966.

Wong, S. F., M. J. W. Boness, and G. J. Schulz, Vibrational Excitation of O_2 by Electron Impact above 4 eV, Phys. Rev. Letters, 31, 969, 1973.

Young, T. R., and J. P. Boris, A Numerical Technique for Solving Stiff Ordinary Differential Equations Associated with Reactive-Flow Problems, NRL Memorandum Report 2611, Naval Research Laboratory, Washington, D.C.

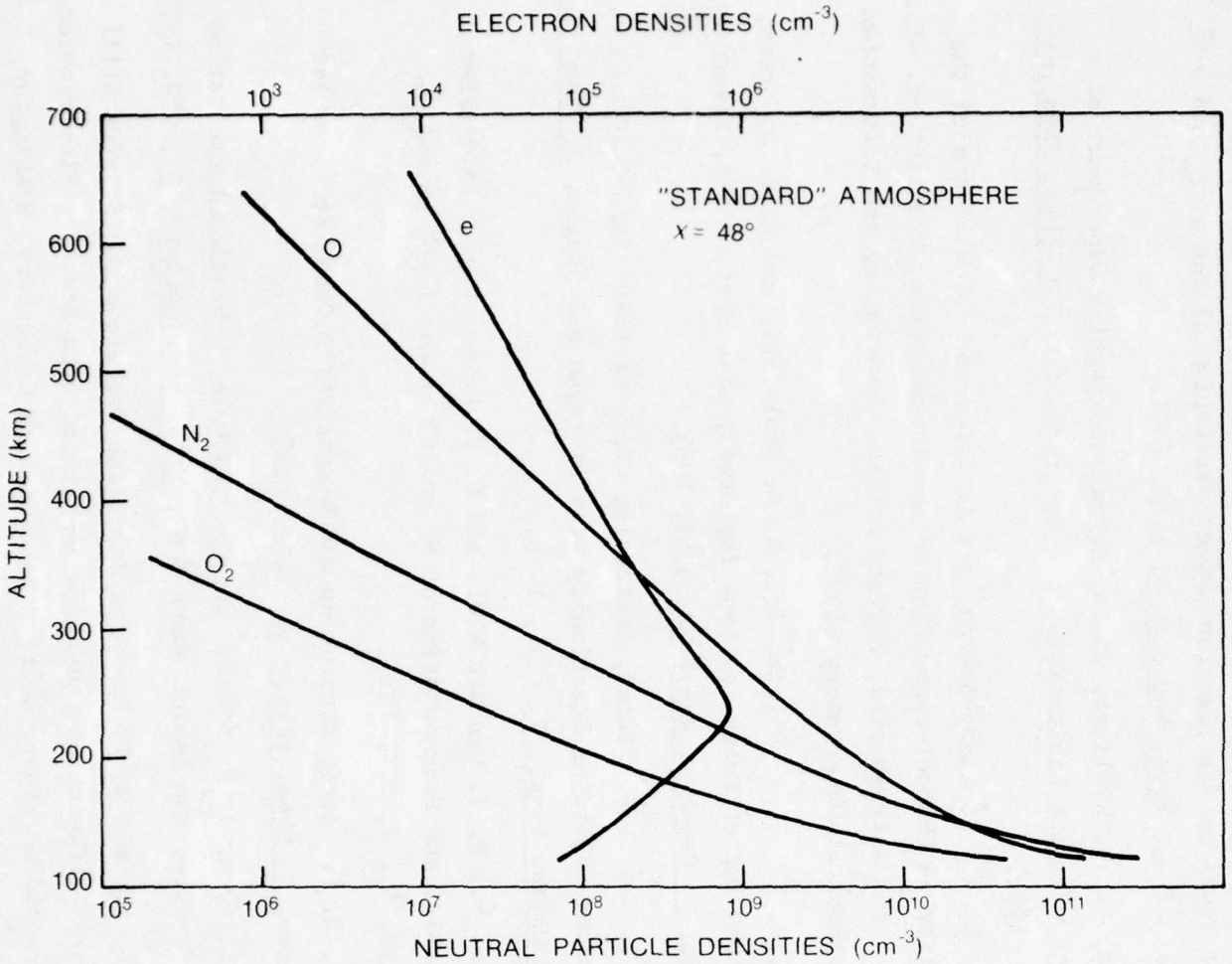

Fig. 1 — Neutral atmosphere and electron density model for the "standard" calculation at $\chi = 48^{\circ}$

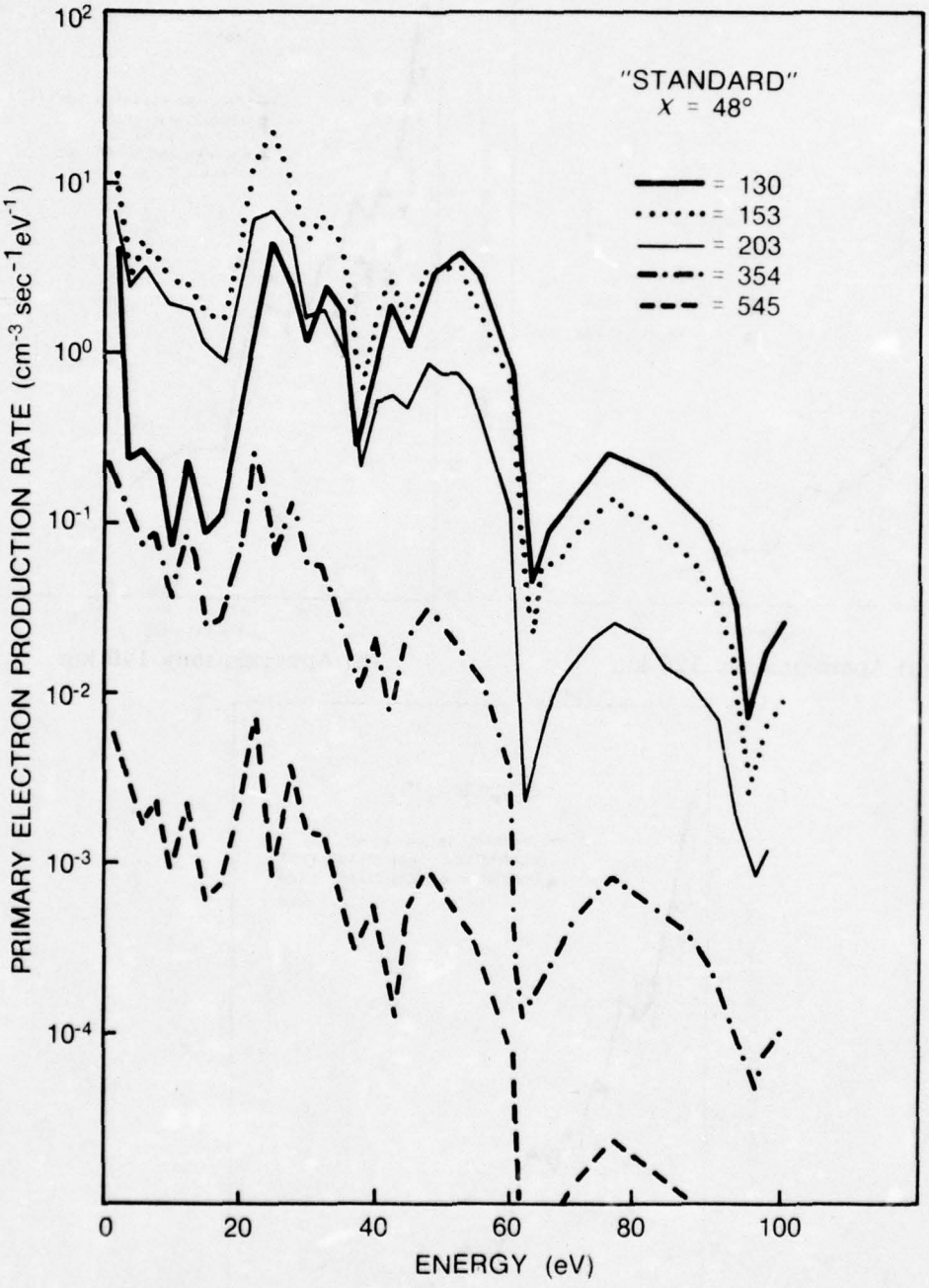

Fig. 2 — Primary electron production rate at selected altitudes for standard calculation

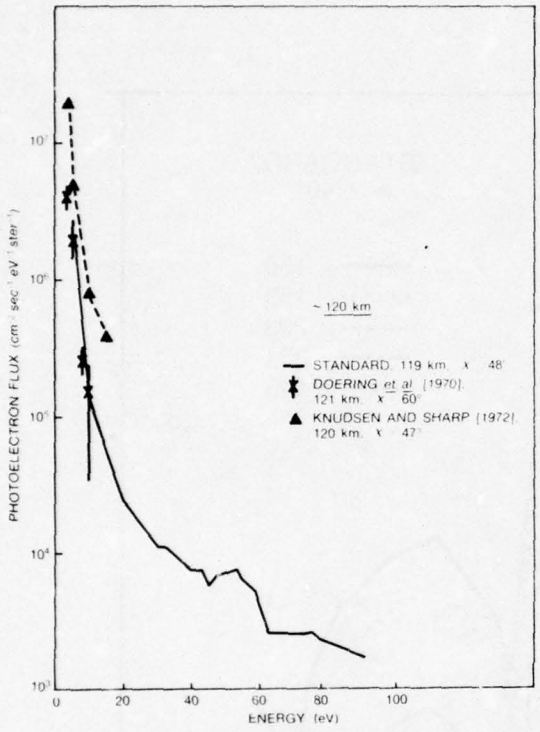

(a) Approximately 120 km

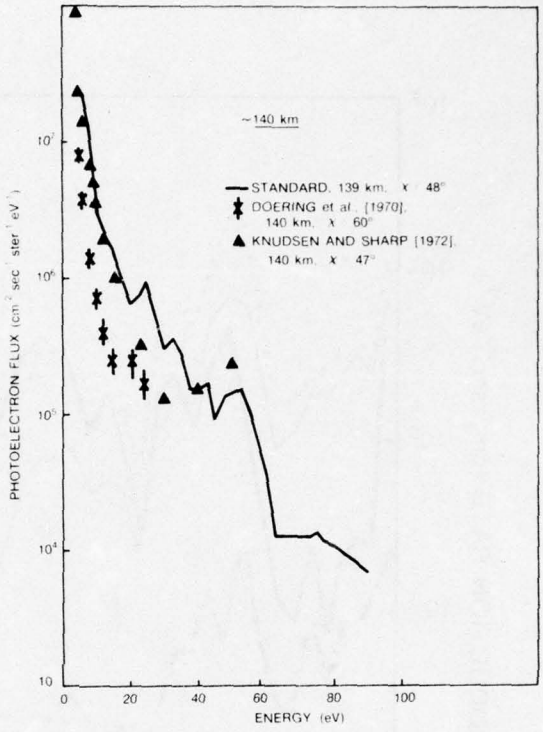

(b) Approximately 140 km

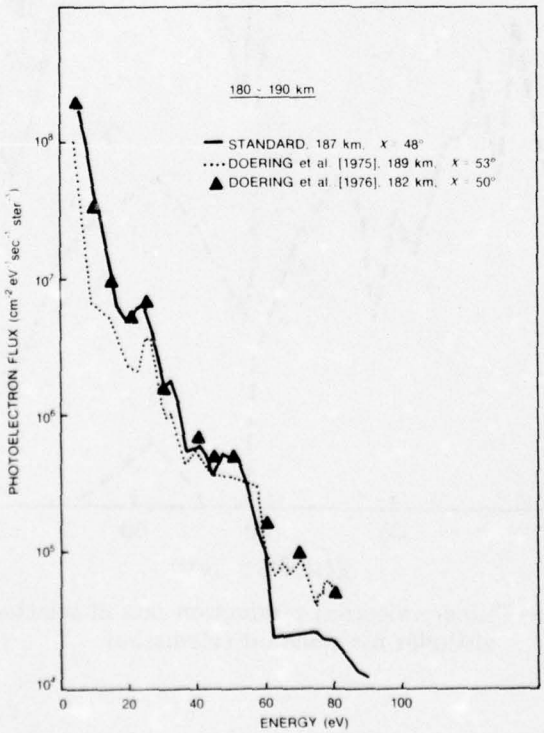

(c) 180-190 km

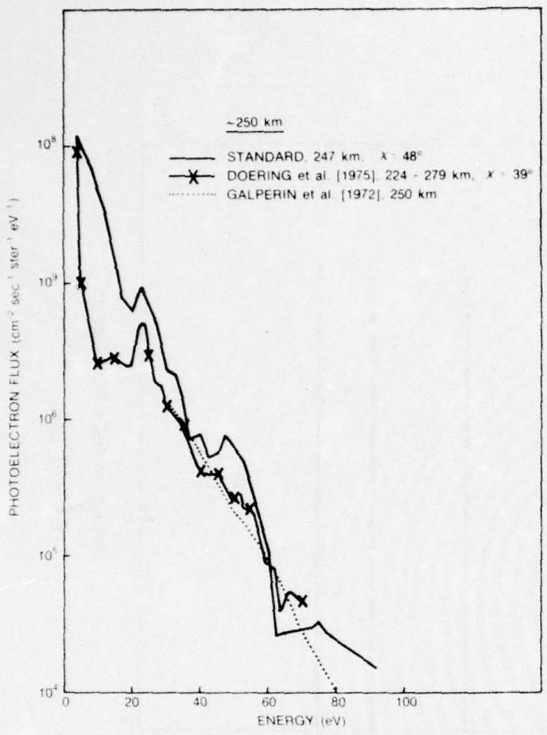

(d) Approximately 250 km

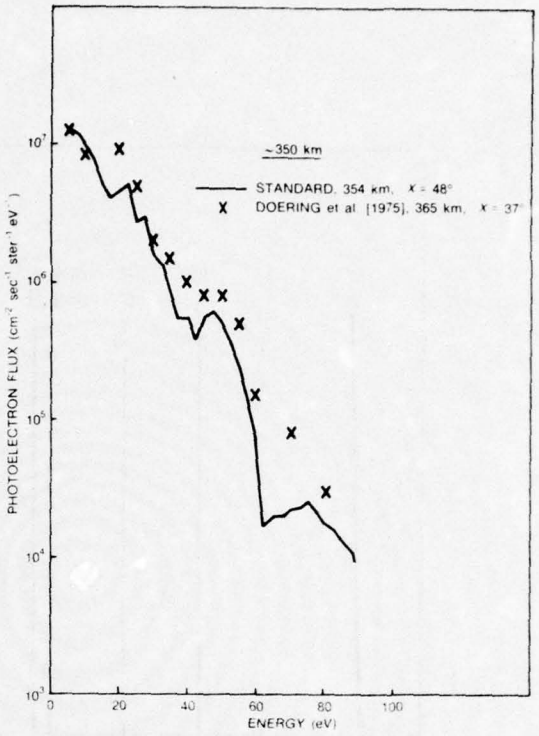

(e) Approximately 350 km

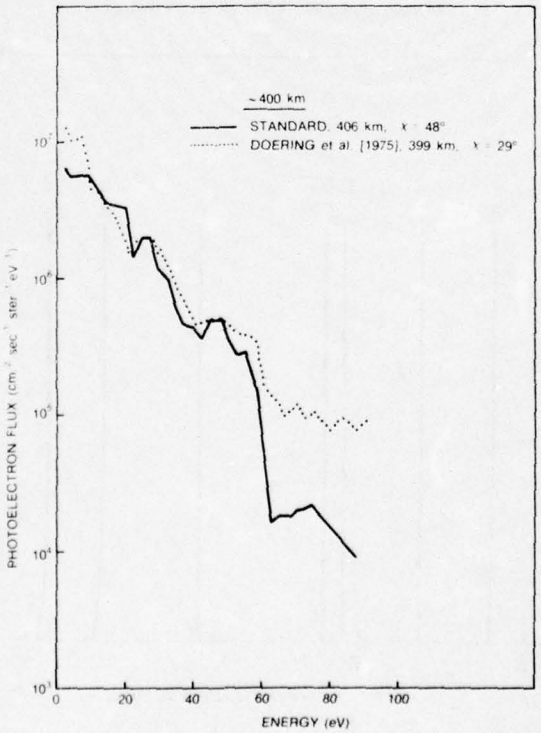

(f) Approximately 400 km

Fig. 3 — Comparison of the photoelectron fluxes from the standard calculation to measured fluxes at selected altitudes

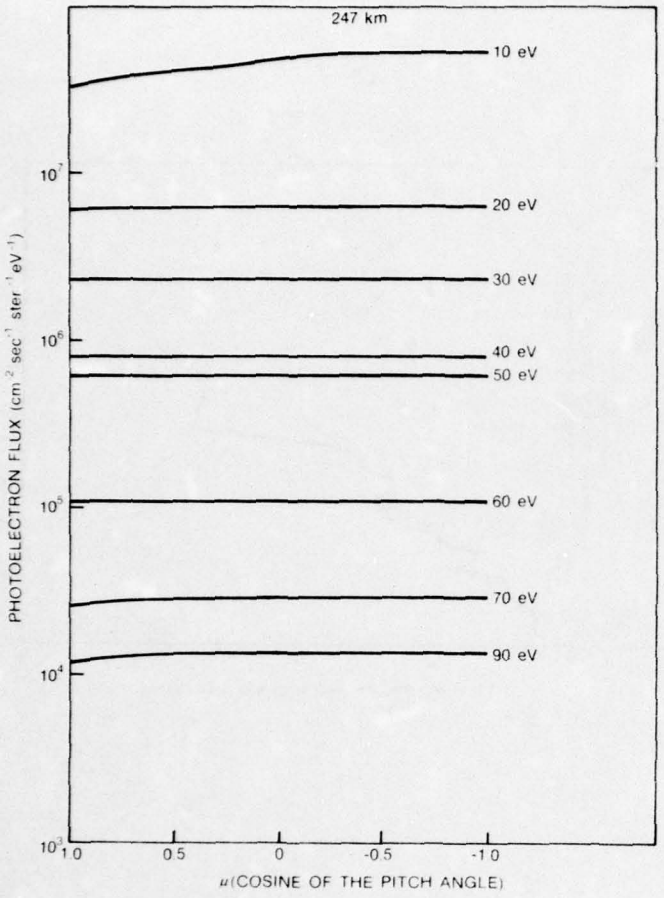

(a) 187 km

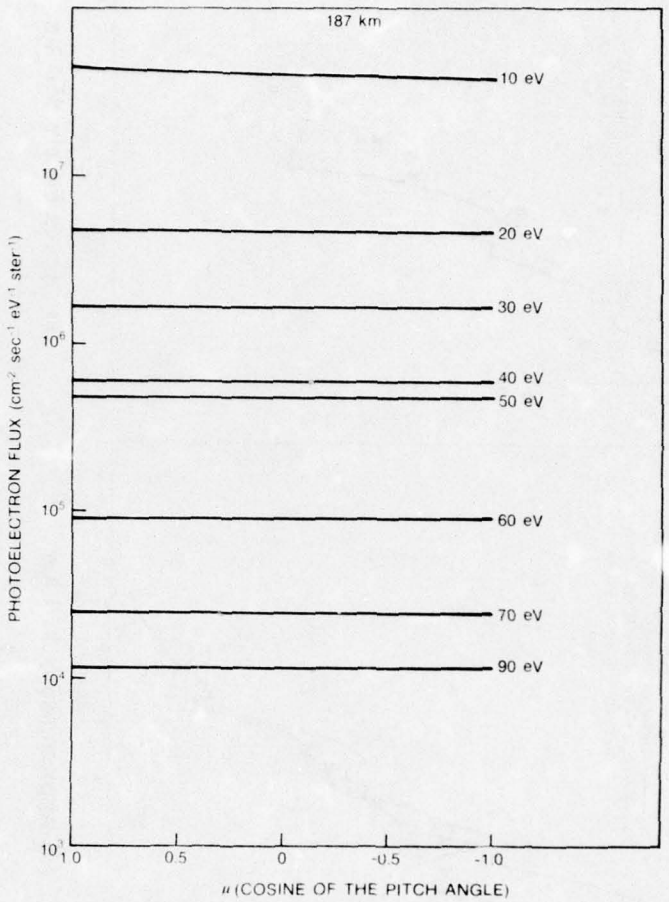

(b) 247 km

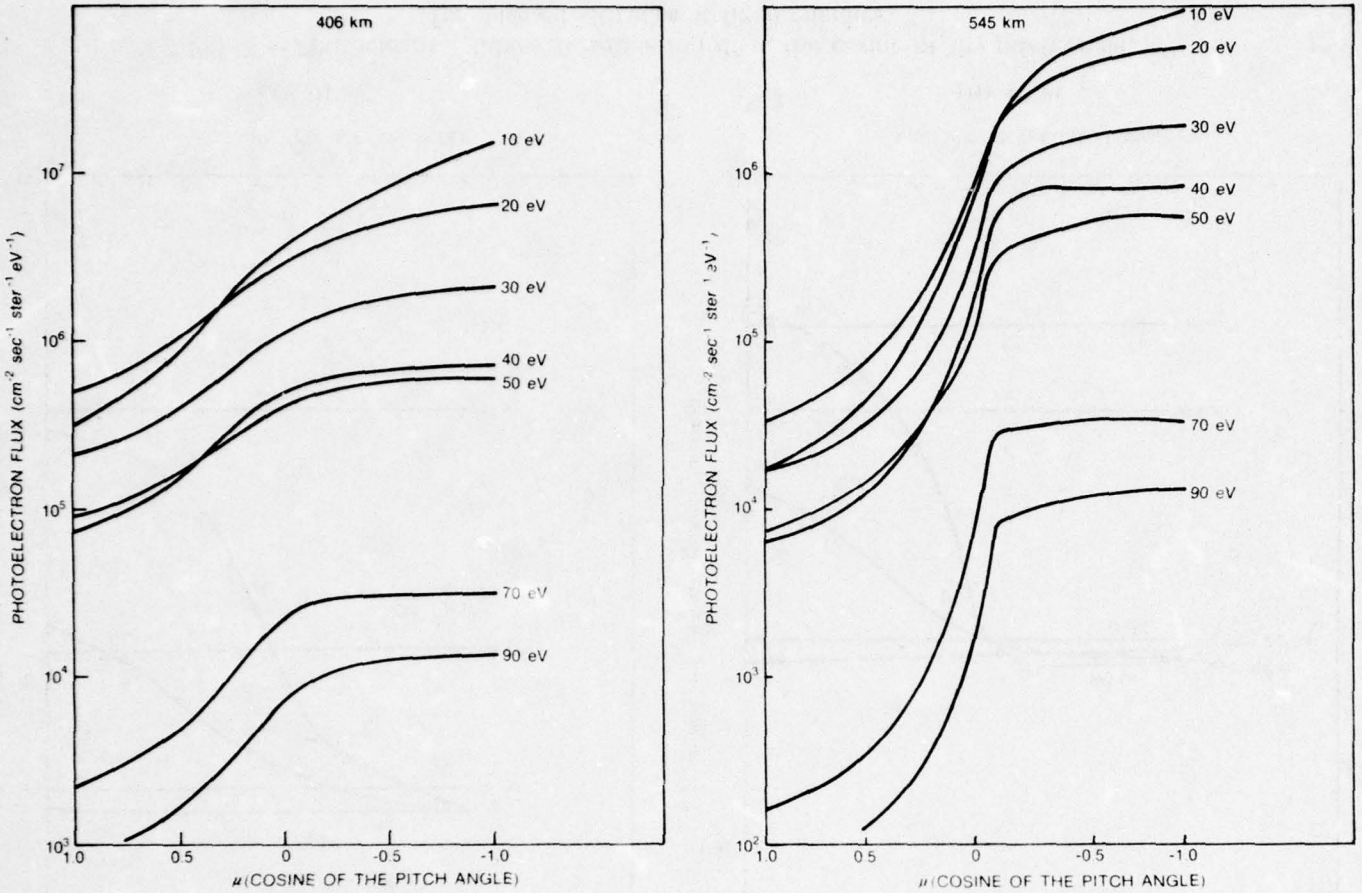

(c) 406 km

(d) 545 km

Fig. 4 — Photoelectron fluxes as a function of μ, the cosine of the pitch angle, for selected energies at fixed altitudes. Note that + 1 is down and -- 1 is up.

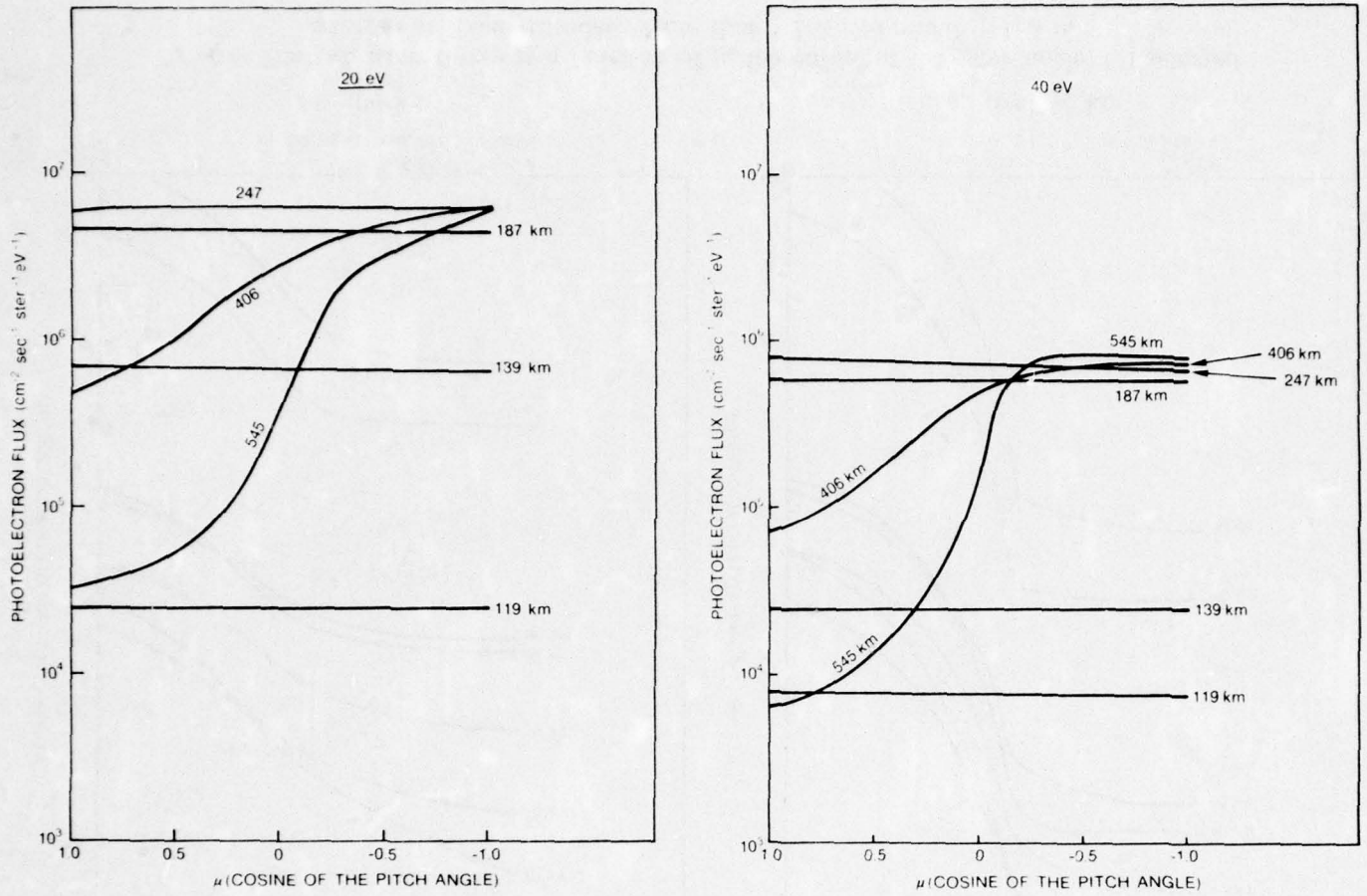

(a) 20 ev

(b) 40 ev

Fig. 5 — Photoelectron fluxes as a function of μ, the cosine of the pitch angle, for selected altitudes at fixed energies

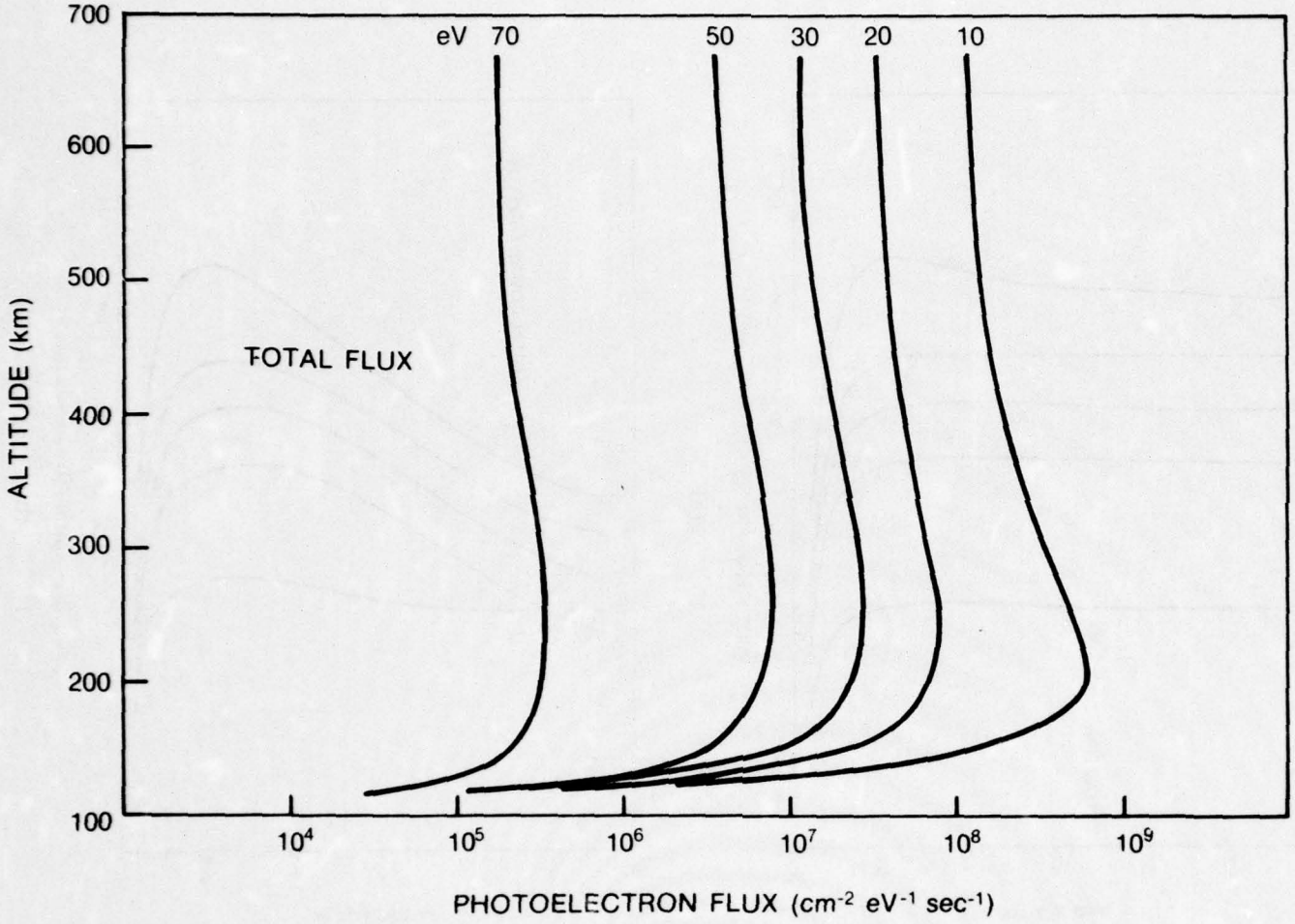

Fig. 6 — Total photoelectron fluxes as a function of altitude for selected energies

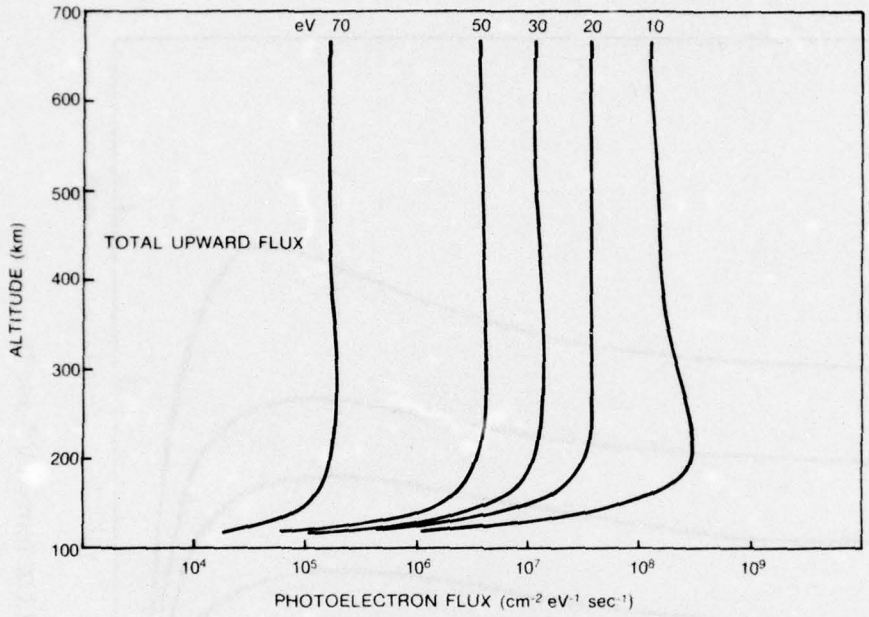

(a)

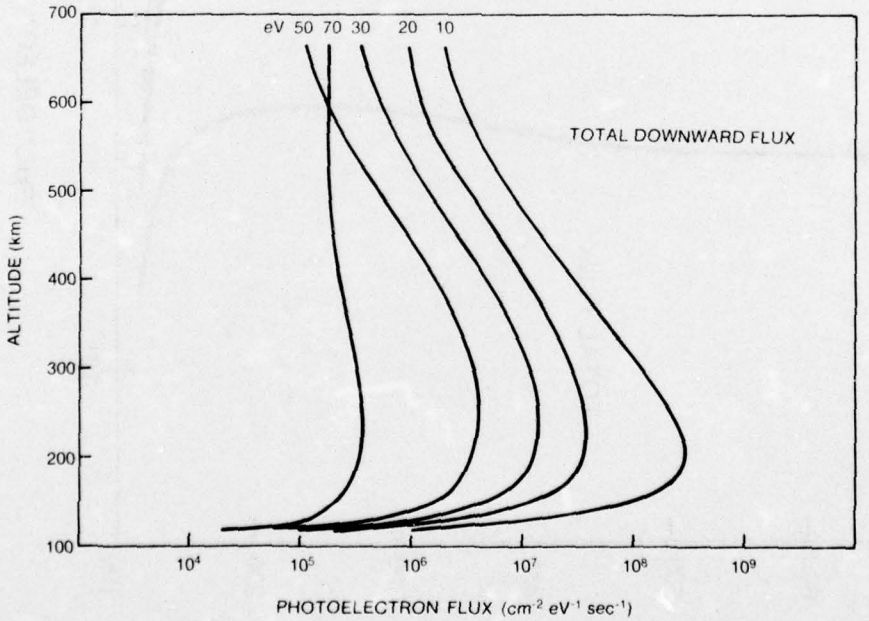

(b)

Fig. 7 — (a) Total upward photoelectron fluxes as a function of altitude for selected energies, (b) total downward photoelectron fluxes as a function of altitude for selected energies

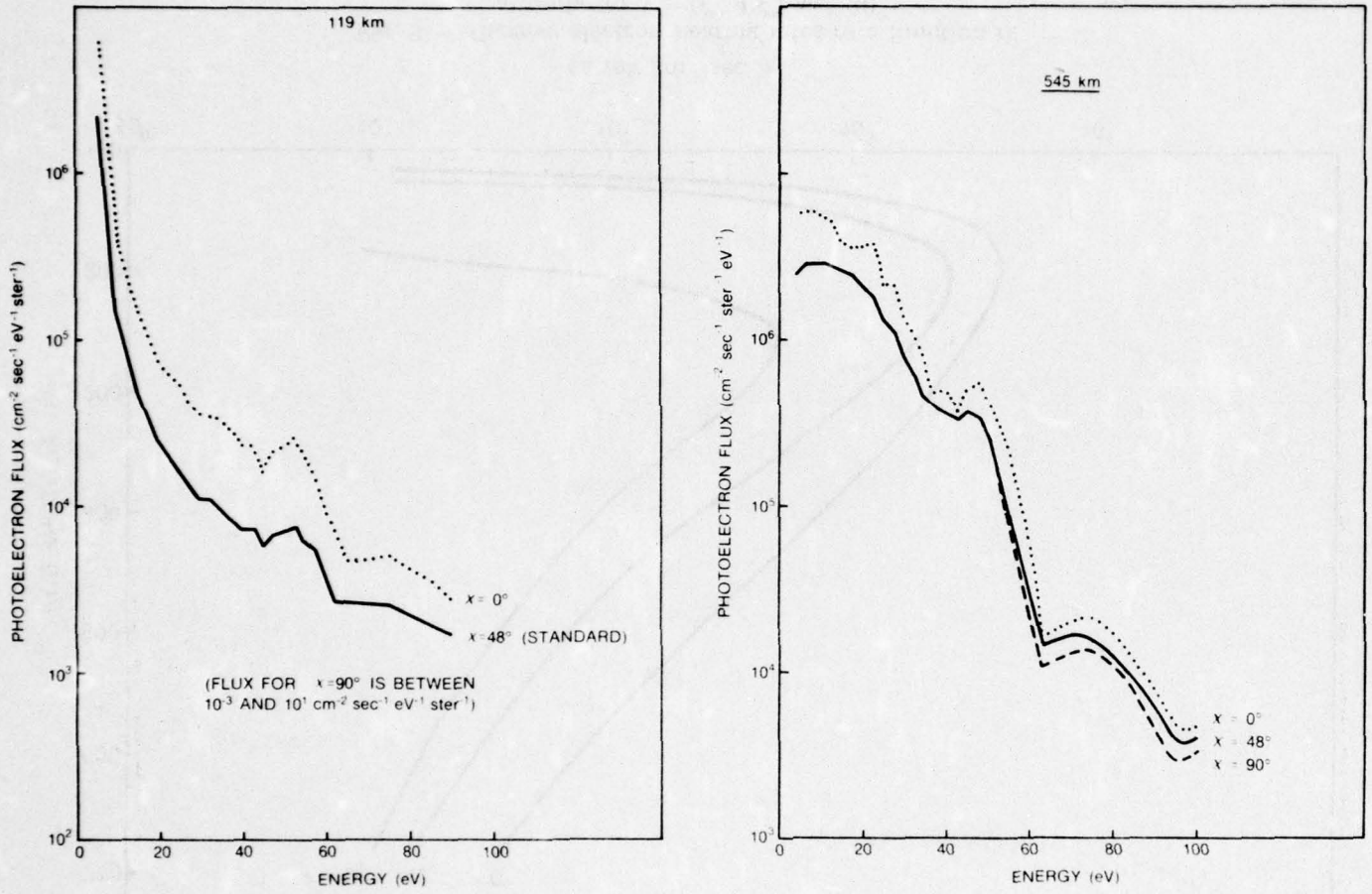

(a) 119 km

(b) 545 km

Fig. 8 — Comparison of photoelectron fluxes as a function of energy for $\chi = 0°$, 48°, and 90° at selected altitudes

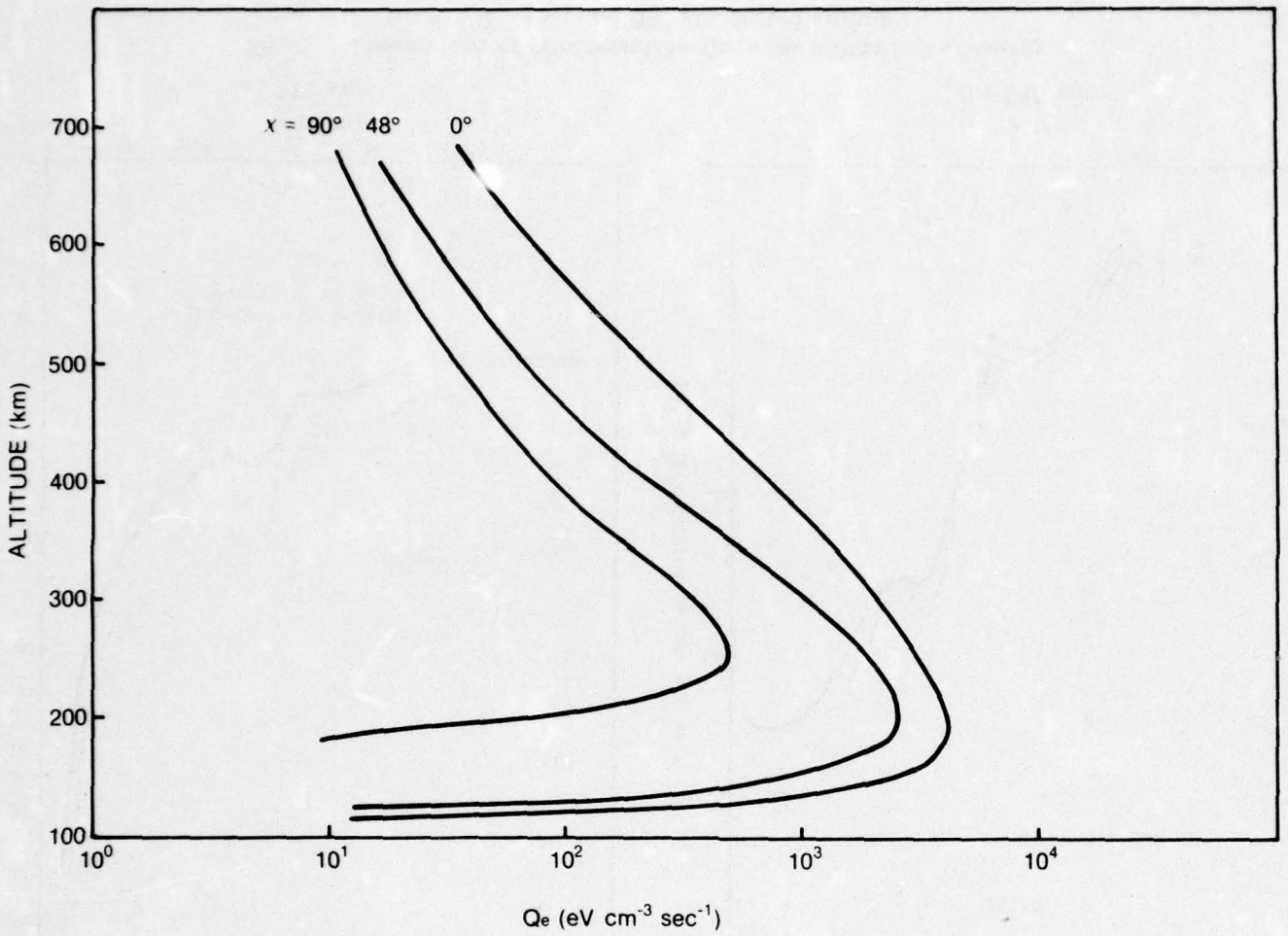

Fig. 9 — Thermal electron heating rates as a function of altitude for $\chi = 0°$, 48°, and 90°

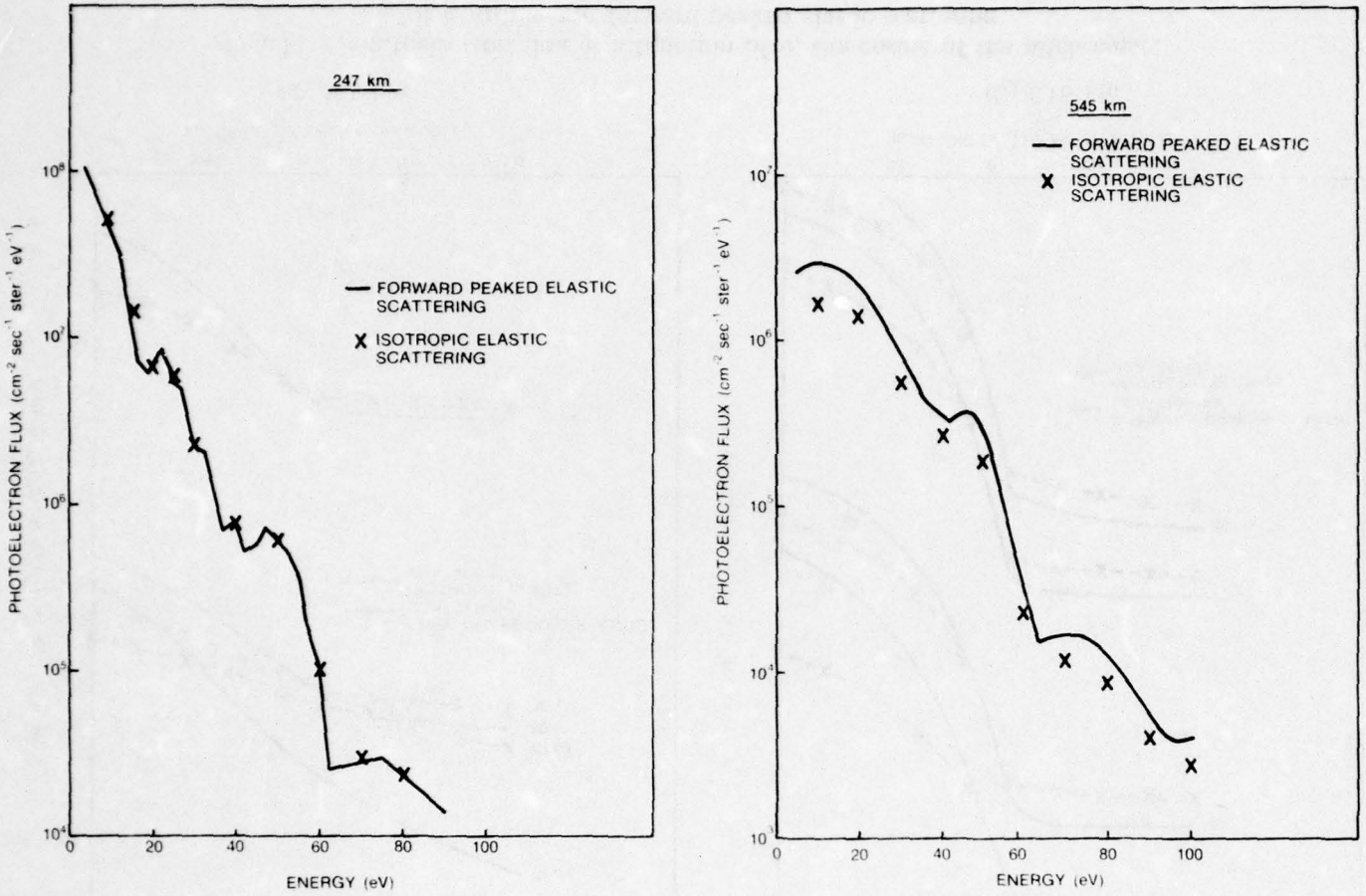

(a) 247 km

(b) 545 km

Fig. 10 — Photoelectron flux as a function of energy for isotropic and forward peaked elastic scattering

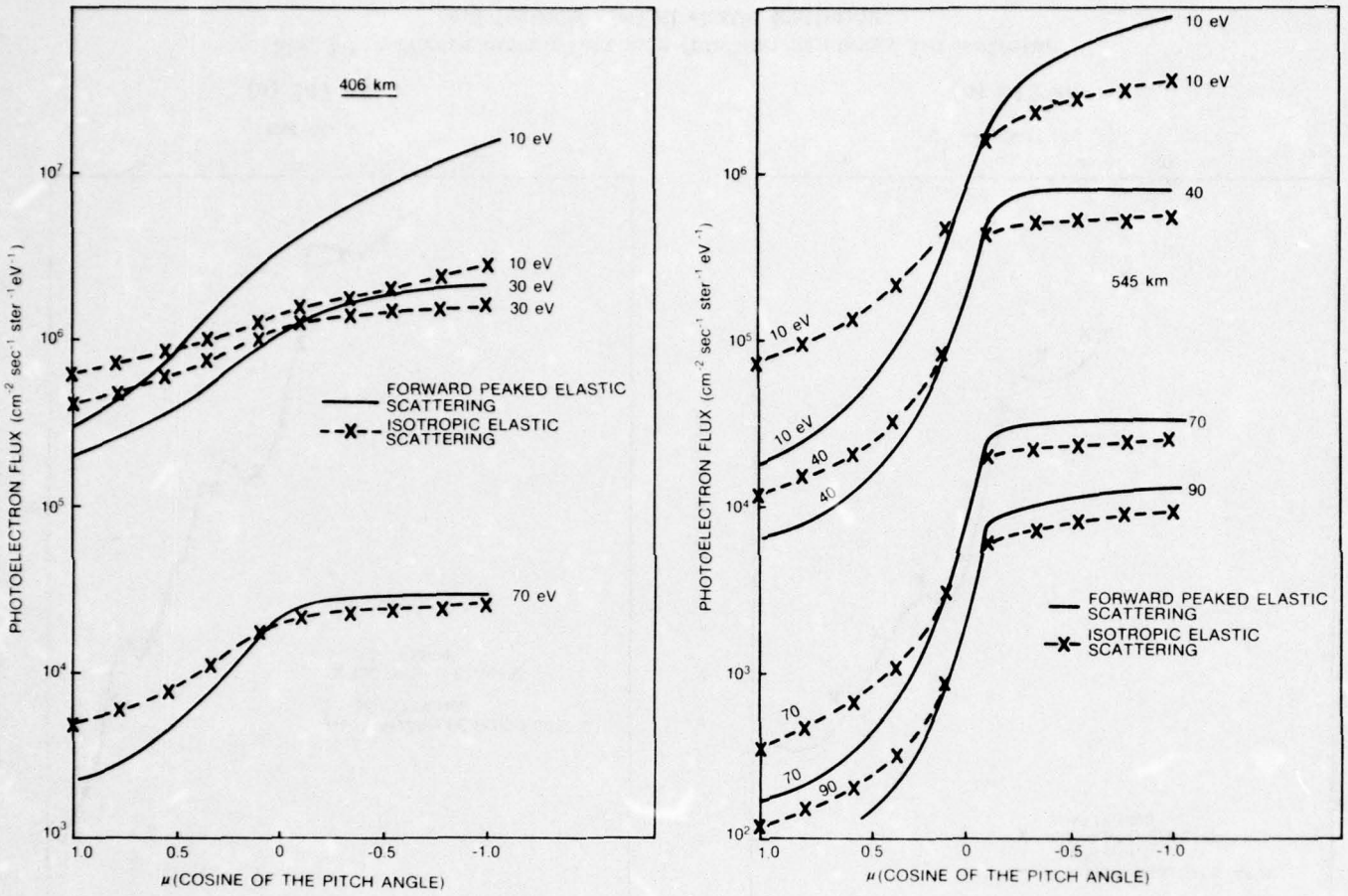

(a) 406 km

(b) 545 km

Fig. 11 — Photoelectron flux as a function of μ, the cosine of the pitch angle, for isotropic and forward peaked elastic scattering

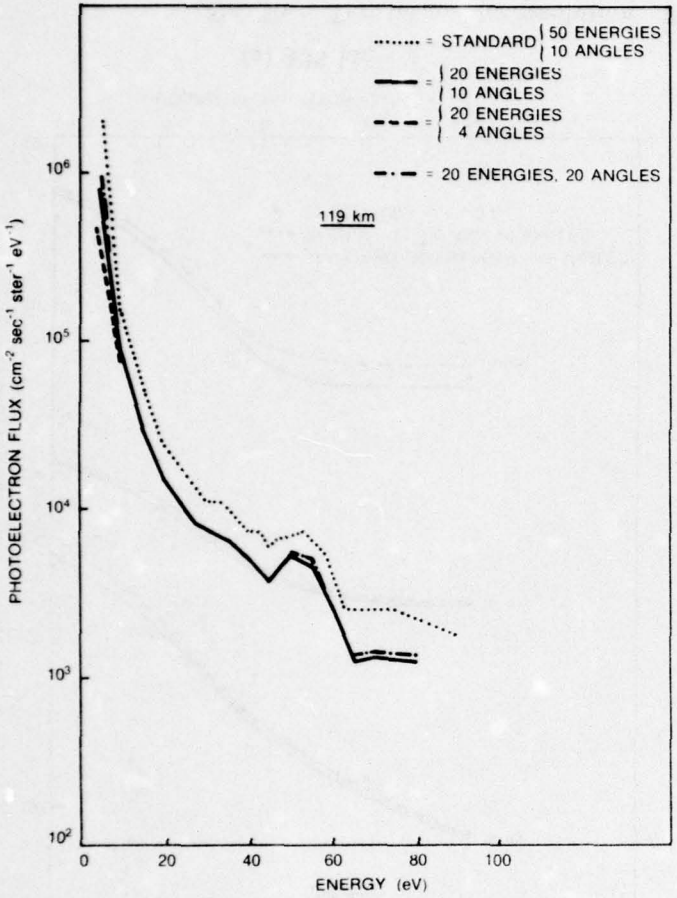

(b) 119 km

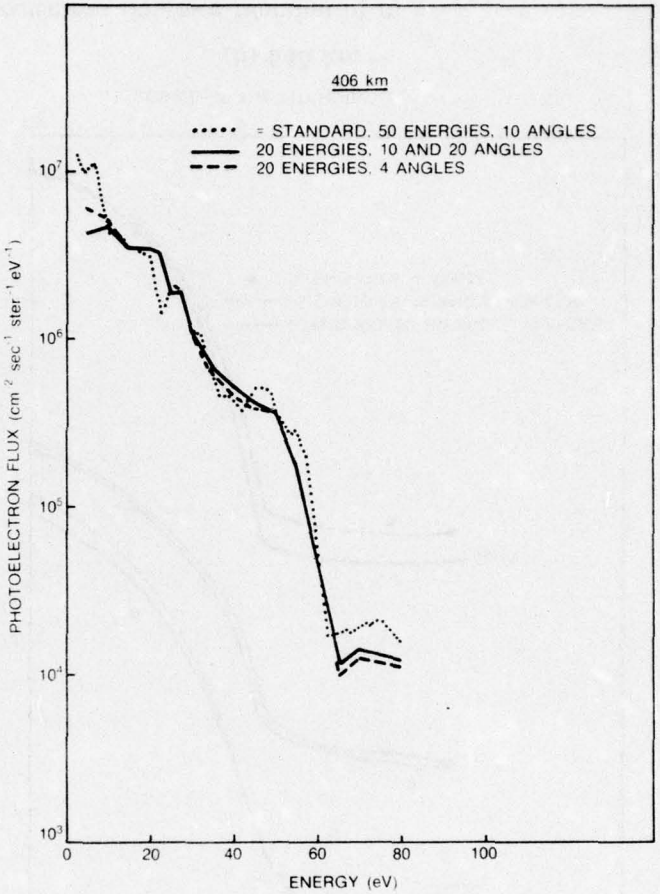

(b) 406 km

Fig. 12 — Test of angular resolution. Photoelectron flux as a function of energy.

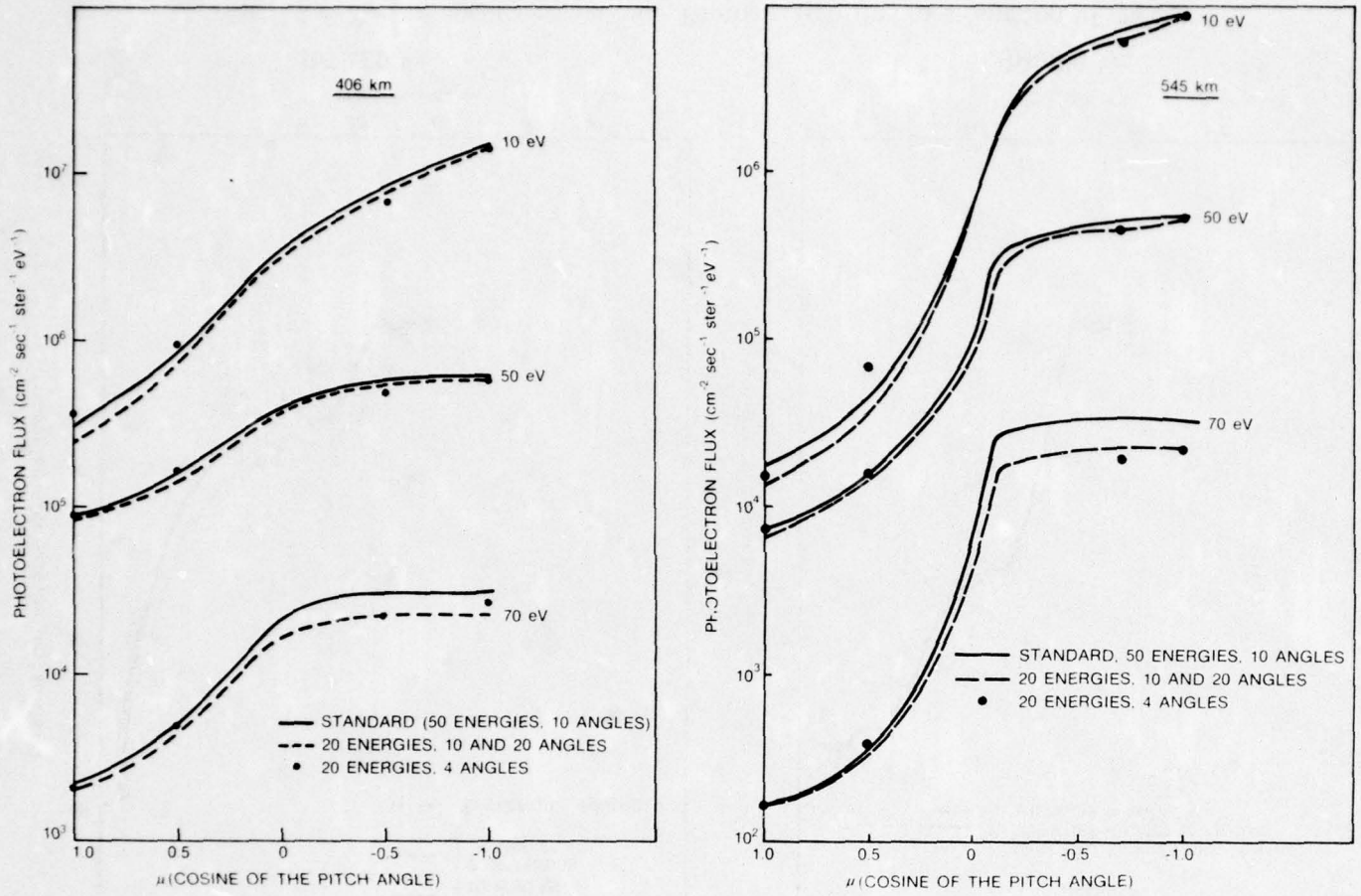

(a) 406 km

(b) 545 km

Fig. 13 — Test of angular resolution. Photoelectron flux as a function of μ, the cosine of the pitch angle, at selected energies.

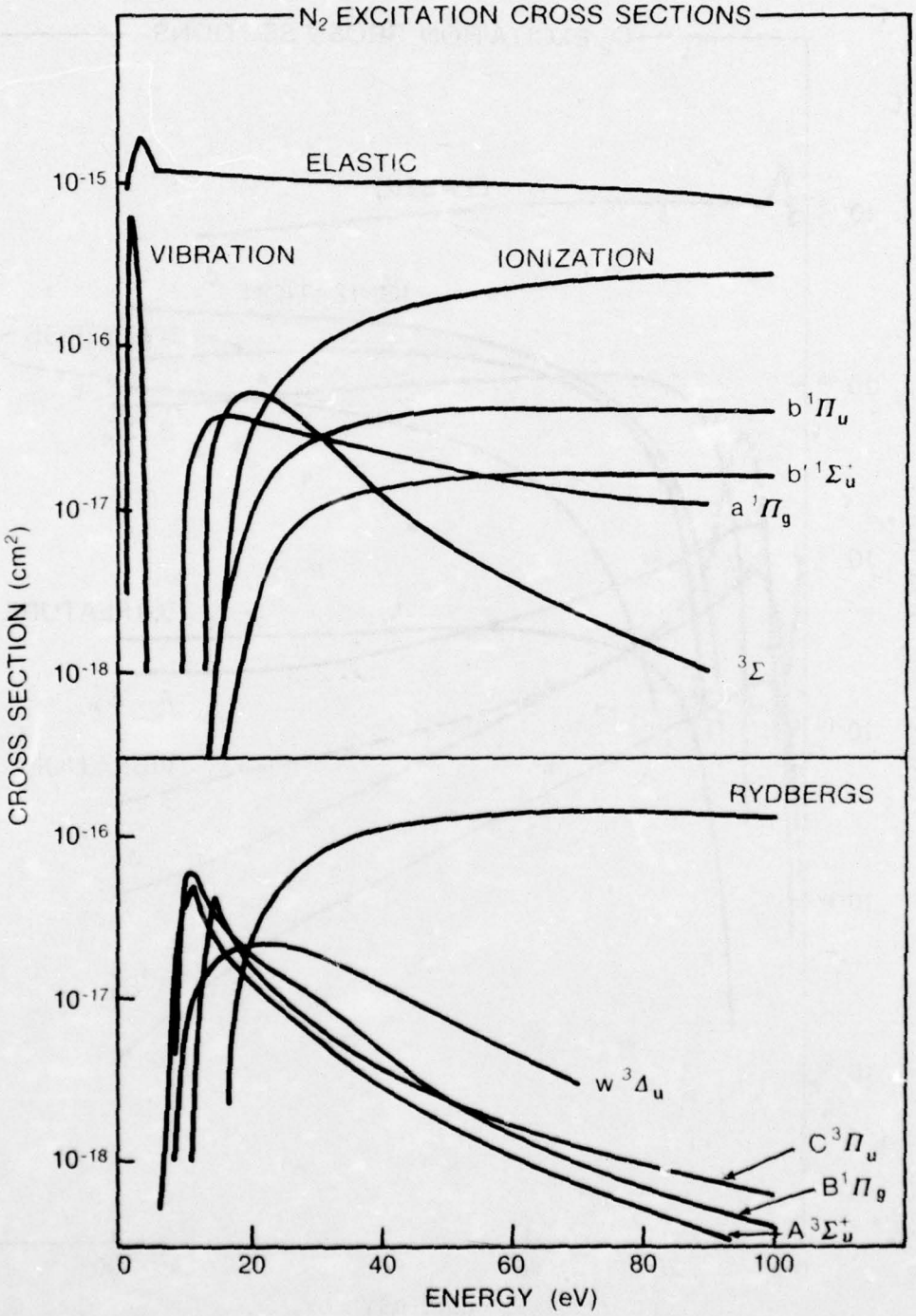

Fig. 14 — Electron impact excitation cross sections for N_2

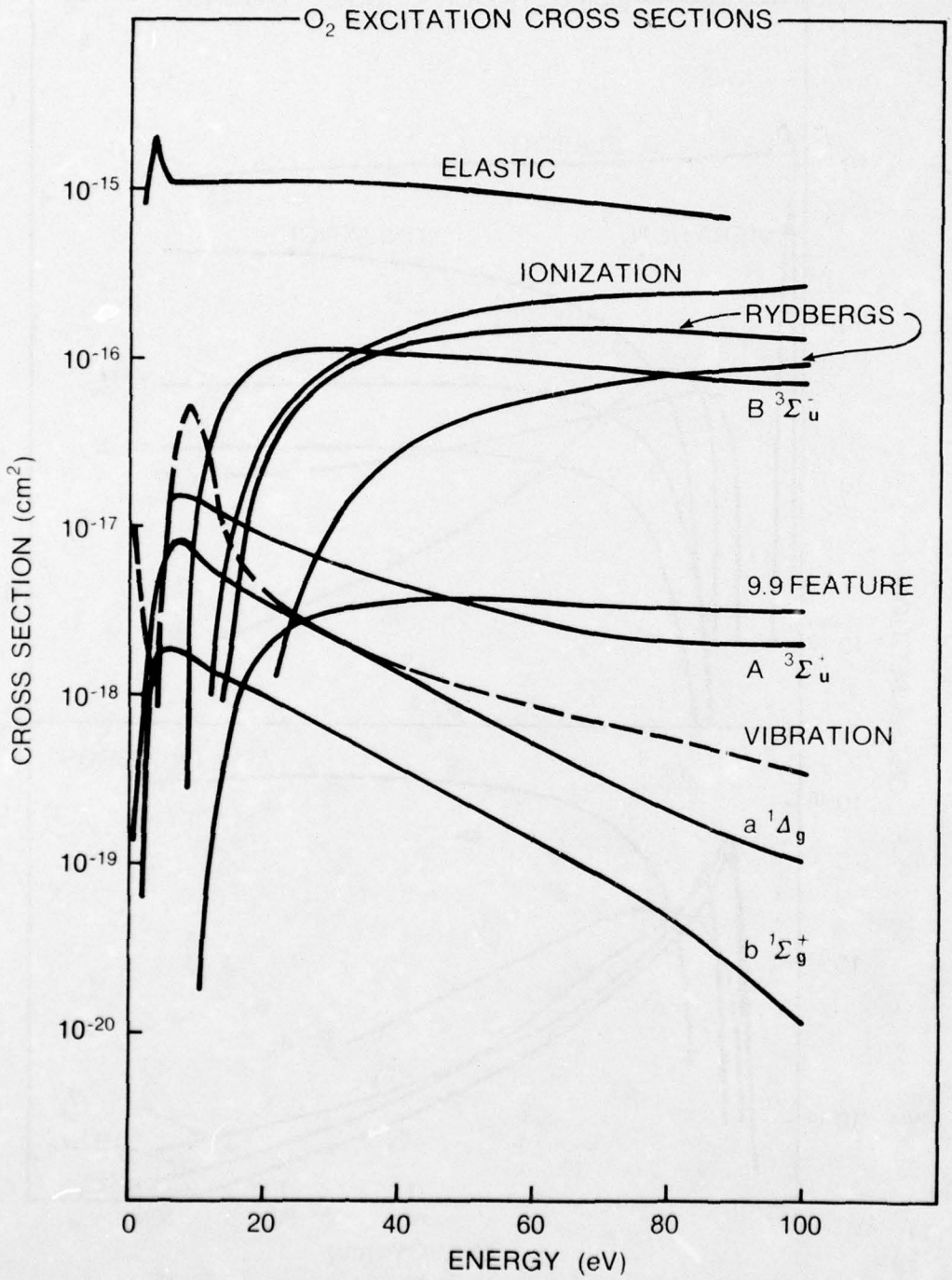

Fig. 15 — Electron impact excitation cross sections for O_2

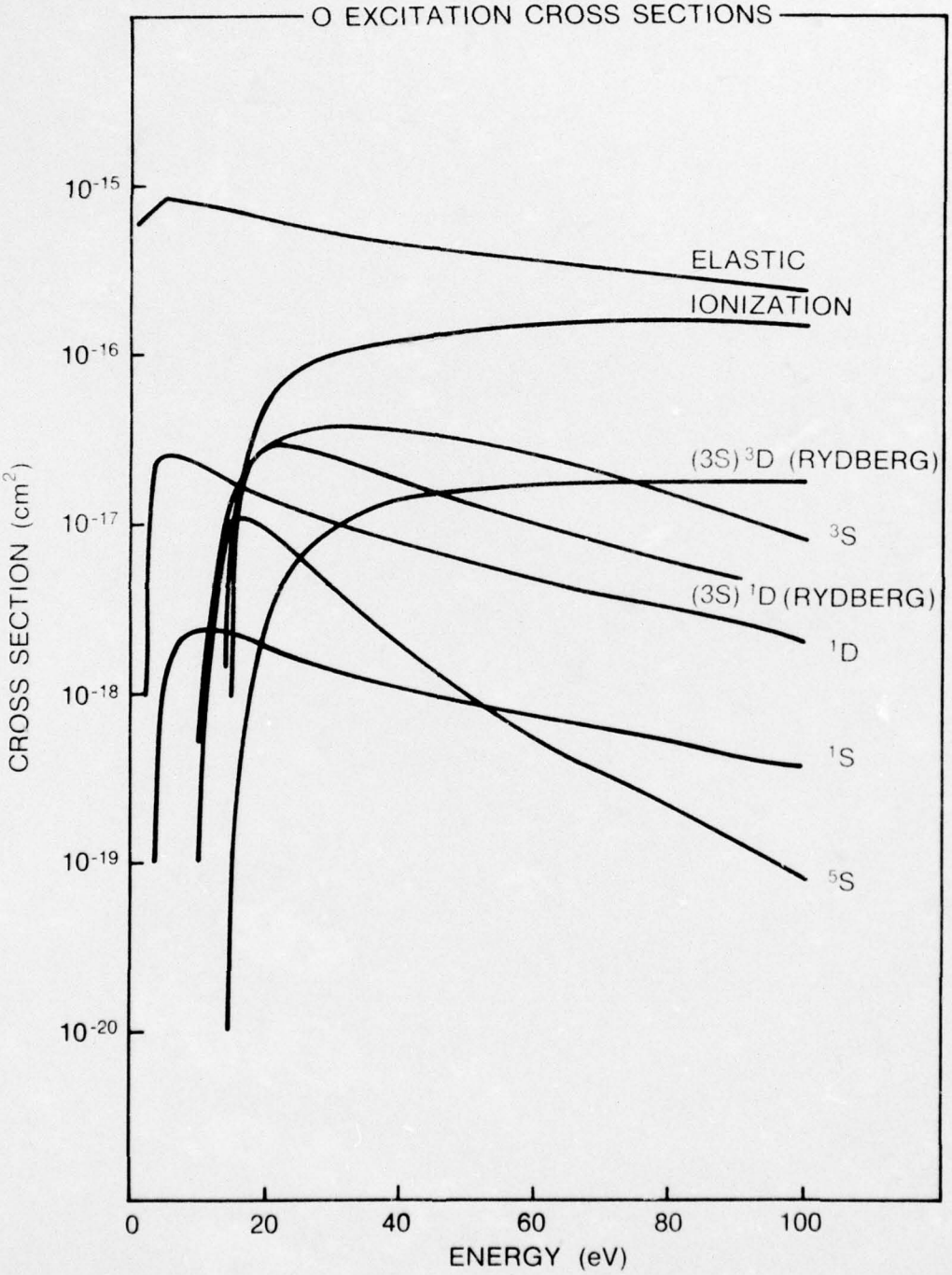

Fig. 16 — Electron impact excitation cross sections for O